Protein Science (1996), *5*:2054–2073. Cambridge University Press. Printed in the USA.

Modeling of the D1/D2 proteins and cofactors of the photosystem II reaction center: Implications for herbicide and bicarbonate binding

JIN XIONG,[1] SHANKAR SUBRAMANIAM,[2,3] AND GOVINDJEE[1,2]

[1]Department of Plant Biology, University of Illinois at Urbana-Champaign, Urbana, Illinois 61801
[2]Center for Biophysics and Computational Biology, University of Illinois at Urbana-Champaign, Urbana, Illinois 61801
[3]Beckman Institute, University of Illinois at Urbana-Champaign, Urbana, Illinois 61801

(RECEIVED May 7, 1996; ACCEPTED July 30, 1996)

Abstract

A three-dimensional model of the photosystem II (PSII) reaction center from the cyanobacterium *Synechocystis* sp. PCC 6803 was generated based on homology with the anoxygenic purple bacterial photosynthetic reaction centers of *Rhodobacter sphaeroides* and *Rhodopseudomonas viridis*, for which the X-ray crystallographic structures are available. The model was constructed with an alignment of D1 and D2 sequences with the L and M subunits of the bacterial reaction center, respectively, and by using as a scaffold the structurally conserved regions (SCRs) from bacterial templates. The structurally variant regions were built using a novel sequence-specific approach of searching for the best-matched protein segments in the Protein Data Bank with the "basic local alignment search tool" (Altschul SF, Gish W, Miller W, Myers EW, Lipman DJ, 1990, *J Mol Biol 215*:403–410), and imposing the matching conformational preference on the corresponding D1 and D2 regions. The structure thus obtained was refined by energy minimization. The modeled D1 and D2 proteins contain five transmembrane α-helices each, with cofactors (4 chlorophylls, 2 pheophytins, 2 plastoquinones, and a non-heme iron) essential for PSII primary photochemistry embedded in them. A β-carotene, considered important for PSII photoprotection, was also included in the model. Four different possible conformations of the primary electron donor P680 chlorophylls were proposed, one based on the homology with the bacterial template and the other three on existing experimental suggestions in literature. The P680 conformation based on homology was preferred because it has the lowest energy. Redox active tyrosine residues important for $P680^+$ reduction as well as residues important for PSII cofactor binding were analyzed. Residues involved in interprotein interactions in the model were also identified. Herbicide 3-(3,4-dichlorophenyl)-1,1-dimethylurea (DCMU) was also modeled in the plastoquinone Q_B binding niche using the structural information available from a DCMU-binding bacterial reaction center. A bicarbonate anion, known to play a role in PSII, but not in anoxygenic photosynthetic bacteria, was modeled in the non-heme iron site, providing a bidentate ligand to the iron. By modifying the previous hypothesis of Blubaugh and Govindjee (1988, *Photosyn Res 19*:85–128), we modeled a second bicarbonate and a water molecule in the Q_B site and we proposed a hypothesis to explain the mechanism of Q_B protonation mediated by bicarbonate and water. The bicarbonate, stabilized by D1-R257, donates a proton to Q_B^{2-} through the intermediate of D1-H252; and a water molecule donates another proton to Q_B^{2-}. Based on the discovery of a "water transport channel" in the bacterial reaction center, an analogous channel for transporting water and bicarbonate is proposed in our PSII model. The putative channel appears to be primarily positively charged near Q_B and the non-heme iron, in contrast to the polarity distribution in the bacterial water transport channel. The constructed model has been found to be consistent with most existing data.

Keywords: β-carotene; bicarbonate binding; D1 protein; D2 protein; diuron (DCMU); homology modeling; non-heme iron; P680; pheophytin; photosystem II reaction center; plastoquinones Q_A and Q_B; Q_B protonation; *Synechocystis* sp. PCC 6803; tyrosines Z and D

Reprint requests to: Govindjee, Department of Plant Biology, 265 Morrill Hall, 505 S. Goodwin Ave., University of Illinois at Urbana-Champaign, Urbana, Illinois 61801-3707; e-mail: gov@uiuc.edu.

Abbreviations: ABNR, adopted basis Newton Raphson energy minimization approach; BLAST, basic local alignment search tool; DCMU, 3-(3,4-dichlorophenyl)-1,1-dimethylurea; ENDOR, electron nuclear double resonance; EPR, electron paramagnetic resonance; LD, linear dichroism; P680, the primary electron donor of photosystem II; PCC, Pasteur culture collection; PDF, probability density functions method for protein structure refinement and evaluation; PSI, photosystem I; PSII photosystem II; Q_A, the primary plastoquinone electron acceptor of photosystem II; Q_B, the secondary plastoquinone electron acceptor of photosystem II; SCR, structurally conserved region.

The primary photosynthetic reactions of plants, algae, and cyanobacteria occur in photosystem II and photosystem I protein complexes located in thylakoid membranes. The study of the photochemical mechanism of PSII has been a focus of photosynthesis research because this protein complex is the only one in nature that is able to evolve oxygen by splitting water (Renger, 1993). The PSII reaction center lies at the core of the PSII protein complex and carries out the chemical reactions, including the primary charge separation at the reaction center chlorophylls (P680) and a subsequent electron transfer from water to plastoquinone via a number of redox active intermediates, while releasing oxygen as a byproduct (for reviews see Vermaas et al., 1993; Diner & Babcock, 1996). The photochemically active PSII reaction center contains six polypeptides, D1, D2, a heterodimer of cytochrome b_{559}, *psbI*, and *psb*W gene products (see e.g., Satoh, 1993; Lorkovic et al., 1995). The central core of the PSII reaction center is composed of D1 and D2 proteins where all the redox active components are embedded. These components include a tetra-manganese cluster, two redox active tyrosine residues, four to six chlorophyll *a* molecules, two pheophytins, and plastoquinones Q_A and Q_B. A non-heme iron, located between Q_A and Q_B, does not participate directly in the electron transfer, but is vital for the transfer process. A β-carotene is also found in the PSII reaction center and is believed to be involved in the photoprotective process.

An X-ray structure of the PSII reaction center is not available to this date. However, low-resolution electron microscopy structures are available (Holzenburg et al., 1993; Santini et al., 1994; Boekema et al., 1995). Significant sequence and functional homology is known to exist between the PSII reaction center proteins D1 and D2 and the L and M subunits of the photosynthetic reaction centers of purple bacteria *Rhodobacter* (*Rb.*) *sphaeroides* and *Rhodopseudomonas* (*Rps.*) *viridis* (see review by Diner & Babcock, 1996), for which high-resolution crystal structures are available (see review by Lancaster et al., 1995). It is, thus, of considerable interest to construct a reasonable working model for the PSII reaction center, based on the homology with bacterial reaction centers. The availability of the PSII three-dimensional model will enable accurate structural interpretation of experimental data, be useful for proposing functional hypotheses for the electron transfer mechanism, and for suggesting designs of site-directed mutants for elucidating the structure–function relationship in PSII.

Several attempts have already been made to construct a three-dimensional model for the PSII reaction center. Trebst (1986) first aligned the D1 and D2 sequences of the higher plant PSII reaction center with the L and M sequences of the bacterial reaction center and used the homology information to predict the folding of D1 and D2. Based on the model, he also proposed important residues involved in Q_B and the non-heme iron binding. Bowyer et al. (1990) constructed a model (using the sequence from *Synechococcus* 7942) for the Q_B and herbicide-binding niche in the D1 protein, by digitizing the stereoimage of part of the *Rps. viridis* structure. Other Q_B and herbicide-binding niche models have also been constructed by various groups (Tietjen et al., 1991; Ohad et al., 1992; Draber et al., 1993; Egner et al., 1993; Sobolev & Edelman, 1995). Svensson et al. (1990) built a PSII donor side model with the redox active tyrosine residues by using part of the consensus D1/D2 sequences. The model was constructed by replacing a small number of side chains in the related region of the L subunit of *Rps. viridis* structure. A more complete spinach PSII model from this group is now available with refined structures for P680, the pheophytins, and the redox active tyrosyl residues (Svensson, 1995; Svensson et al., 1995a, 1995b). Another comprehensive modeling study for pea PSII was presented by Ruffle et al. (1992), who compared sequences of 23 D1, 9 D2, and 8 bacterial L and 8 bacterial M proteins, and showed a strong sequence similarity among them, especially in the transmembrane regions. An environment-dependent substitution table was applied in the sequence alignment, and the structurally conserved regions of D1, D2, and the bacterial L and M subunits were identified. Using SYBYL molecular modeling package, a partial (73% complete) PSII reaction center model was generated from pea D1 and D2 sequences. With this pea PSII model, Mackay and O'Malley (1993a, 1993b, 1993c, 1993d) conducted a series of herbicide-binding analyses. Their calculations on the intermolecular interactions of several herbicides (e.g., 3-(3,4-dichlorophenyl)-1,1-dimethylurea) with PSII indicate that van der Waals forces play a major role in stabilizing the herbicides in the Q_B niche.

Bicarbonate has been suggested to be a positive regulator for the function of the PSII reaction center (see reviews by Blubaugh & Govindjee, 1988a; Govindjee, 1993; Govindjee & van Rensen, 1993). The depletion of bicarbonate by its analogue formate results in a significant inhibition of the electron transfer on the acceptor side, i.e., from Q_A^- to the plastoquinone pool (see references in Blubaugh & Govindjee, 1988a; Govindjee & van Rensen, 1993). Studies have also suggested that bicarbonate may affect the donor side function of PSII (El-Shintinawy & Govindjee, 1990; Jursinic & Dennenberg, 1990; Stemler & Jursinic, 1993; Klimov et al., 1995; Wincencjusz et al., 1996).

Regarding the role of bicarbonate in PSII function, Michel and Deisenhofer (1988) suggested that bicarbonate may serve as a functional homologue to the glutamate residue in the bacterial reaction center (M232 in *Rps. viridis* numbering), which provides ligands to the non-heme iron. This was based on the finding that there is no homologous glutamate residue in the D1 and D2 sequences, and there is no bicarbonate stimulatory effect in the bacterial system (Shopes et al., 1989). Although the involvement of M232 in the bacterial reaction center as a substitute for bicarbonate could not be confirmed by site-directed mutagenesis experiments (Wang et al., 1992), EPR experiments in PSII confirmed the binding of bicarbonate to the non-heme iron (Diner & Petrouleas, 1990; Petrouleas & Diner, 1990). Further, a hypothesis for the involvement of bicarbonate in the Q_B protonation is supported by other experimental evidence (see Blubaugh & Govindjee, 1988a, Govindjee & van Rensen, 1993). Blubaugh and Govindjee (1988a) presented a hypothesis for the possible involvement of D1-R257 or D1-R269 (with D1-R257 as the more favored residue) in facilitating the bicarbonate-mediated Q_B protonation. Diner et al. (1991b) suggested two patterns of the bicarbonate-iron binding, in which bicarbonate either binds to the iron as a mono- or bidentate ligand. Different ways of bicarbonate liganding to the non-heme iron were also discussed by Govindjee and van Rensen (1993), in which the bicarbonate is stabilized by hydrogen bonding interactions with lysine 265 (pea numbering) in D2. Involvement of other amino acids in this stabilization process has been discussed by Govindjee (1993).

In this paper, we present a complete model of the PSII reaction center of a cyanobacterium *Synechocystis* sp. PCC 6803, including the D1, D2 polypeptides and bound cofactors. We chose to model D1 and D2 of this species because it is one of the most widely used systems for site-directed mutagenesis in photosynthesis (Vermaas, 1993). In our modeling, we take into account the alignment of the SCRs in Ruffle et al. (1992) and use this information in our SCR

alignment of the cyanobacterial D1 and D2 with the L and M subunits. In addition, we modeled the loop regions with a novel sequence-specific approach by searching for the best-matched protein segments in the Protein Data Bank with the "basic local alignment search tool" (Altschul et al., 1990), and fitting the matching fragment conformations onto the corresponding D1 and D2 regions. With the inclusion of all the cofactors important for the PSII functions, a complete model of the central core of the PSII reaction center was constructed and refined through energy minimization. Various issues important in the study of the PSII reaction center, including protein binding environment for the cofactors and residues involved in interprotein interactions, were analyzed. Three alternative conformations of P680 chlorophylls different from that of the bacterial counterparts were also proposed based on various experimental suggestions. For the first time, a β-carotene was included in the PSII reaction center model. Redox active residues important for the $P680^+$ reduction, i.e., D1-Y161 and D2-Y160, have also been studied and their modeled distances to the several cofactors have been shown to match well with the experimental suggestions. This model was further applied to the modeling of herbicide DCMU in the Q_B binding niche. We focus in our modeling on the bicarbonate binding and its function in photosystem II. A bicarbonate anion was modeled in the non-heme iron site, providing a bidentate ligand to the iron. By modifying the previous hypothesis of Blubaugh and Govindjee (1988a), we modeled a second bicarbonate and a water molecule in the Q_B site and we propose a hypothesis to explain the mechanism of Q_B protonation mediated by a bicarbonate and a water molecule, in which the bicarbonate, stabilized by D1-R257, donates a proton to Q_B^{2-} through an intermediate of D1-H252; the water molecule is proposed to donate another proton to the doubly reduced Q_B. Based on the structure of the "water transport channel" in the bacterial reaction center, we propose a similar, but not identical, channel for transporting water and bicarbonate in PSII. Our model indicates a more positively charged binding domain near Q_B and the non-heme iron, in contrast to the situation in the bacterial reaction center, which lacks the bicarbonate effect.

Results and discussion

Sequence alignment and sequence-specific loop modeling

Ruffle et al. (1992), using an environment-dependent substitution table, aligned the bacterial L and M subunits with the D1 and D2 sequences and derived the SCRs for pea D1 and D2. This alignment information for the SCRs, with further refinements, was applied in our D1/D2 alignment of *Synechocystis* sp. PCC 6803 with the bacterial templates.

In contrast to Ruffle et al. (1992), who used all four bacterial subunits as templates, we used two L subunits as homology templates for modeling D1 and two M subunits as templates for D2, based on the long-standing assumption that D1 is the equivalent of L and D2 is the equivalent of M (Trebst, 1986; Michel & Deisenhofer, 1988). We suggest that this option will yield a more reliable sequence alignment because examination of the secondary structure of L and M in loop regions shows significant variations between the L and M subunits. If we had applied the averaged coordinates of all the four template proteins in modeling, we expect that many regions, especially those in between the SCRs, would have had significant errors and structural constraints.

The alignment of the D1 protein with the L subunits of both *Rps. viridis* and *Rb. sphaeroides* is shown in Figure 1. After alignment, we find 20% sequence identity (69 identical residues) and 60% sequence similarity of D1 with the L subunit (205 similar residues). The alignment of D2 with the M subunit sequences is shown in Figure 2. After alignment, the sequence identity of D2 with the M subunit is 24% (85 identical residues) and the sequence similarity is 58% (204 similar residues). Because template structures were well characterized and our sequence alignment is based on the homology of the three-dimensional structures, we counted the homology with either of the template sequences. This is a standard protocol followed in family sequence alignments based on structural criteria. However, if the homology is counted with both of the template sequences, both the identity and similarity values will be lower than noted above.

The loop regions, which represent insertion sequences, were modeled using a bits-and-pieces sequence homology modeling strategy. The loop regions are presumably all solvent exposed; it is thus justifiable to use structural fragments from other proteins, even soluble proteins, because loop regions are well characterized by sequences (Han & Baker, 1996). This was done by searching for highly homologous sequences in proteins whose high-resolution structures are available. The search was done using a "basic local alignment search tool" (Altschul et al., 1990). Table 1 gives sequences from highly resolved structures that are homologous to the D1 and D2 loop sequences. In all the hits, the smallest Poisson probability is above 0.95; hence the sequence similarity is significant and we copied the fragment structures for homology modeling.

```
SL *1   *ALLSFERKYR*11 *VPGGTLVGGN*21 *LFDFWVGP--*29 *--FYVGFFGV
VL *1   *ALLSFERKYR*11 *VRGGTLIGGD*21 *LFDFWVGP--*29 *--YFVGFFGV
D1 *1   *----mtttlq*7  *qresaslweq*17 *fcq-wvtstn*26 *nriyvgwfgt

SL *37  *ATFFFAALGI*47 *ILIAWSAVLQ*57 *GT------WN*61 *P---------
VL *37  *SAIFFIFLGV*47 *SLIGYAASQG*57 *PT------WD*61 *P---------
D1 *36  *lmiptlltat*46 *tcfiiafiaa*56 *ppvdidgire*66 *pvagsllygn

SL *62  *QLISVY--PP*70 *----ALE-YG*75 *L-GGAPL---*81 *A-KGGLWQII
VL *62  *FAISIN--PP*70 *----DLK-YG*75 *L-GAAPL---*81 *L-EGGFWQAI
D1 *76  *niisgavvps*86 *snaiglhfyp*96 *iweaasldew*106*lynggpyqlv

SL *90  *TICATGAFVS*100*WALREVEICR*110*KLGI-GYHIP*119*FAFAFAILAY
VL *90  *TVCALGAFIS*100*WMLREVEISR*110*KLGI-GWHVP*119*LAFCVPIFMF
D1 *116*vfhfligifc*126*ymgrqwelsy*136*rlgmrpw-ic*145*vaysapvsaa

SL *129*LTLVLFRPVM*139*MGAWGYAFPY*149*GIWTHLDWVS*159*NTGYTYGNFH
VL *129*CVLQVFRPLL*139*LGSWGHAFPY*149*GILSHLDWVN*159*NFGYQYLNWH
D1 *155*tavfliypig*165*qgsfsdgmpl*175*gisgtfnfmi*185*vfqaeh-nil

SL *169*YNPAHMIAIS*179*FFFTNALALA*189*LHGALVLSAA*199*N-------PE
VL *169*YNPGHMSSVS*179*FLFVNAMALG*189*LHGGLILSVA*199*N-------PG
D1 *194*mhpfhmlgva*204*gvfggslfsa*214*mhgslvtssl*224*vrettevesq

SL *202*K-GKE-----*206*----MRTPDH*212*EDTFF-RD-L*220*VGY-S-IGTL
VL *202*D-GDK-----*206*----VKTAEH*212*ENQYF-RD-V*220*VGY-S-IGAL
D1 *234*nygykfgqee*244*etyni---va*251*ahgyfgr-li*260*fqyasfnnsr

SL *228*GIHRLGLLLS*238*LSAVFFSALC*248*MIIT-----G*253*-TI-------
VL *228*SIHRLGLFLA*238*SNIFLTGAFG*248*TIAS-----G*253*-PF-------
D1 *270*slhfflgawp*280*vigiwftamg*290*vstmafnlng*300*fnfnqsilds

SL *255*WFDQWVDWWQ*265*WWVKL--PW-*272*---------W*273*A-NIPGG
VL *255*WTRGWPEWWG*265*WWLDI--PF-*272*---------W*273*S
D1 *310*qgrvigtwad*320*vlnranigfe*330*vmhernahnf*340*pldla
```

Fig. 1. Sequence alignment of the D1 protein of *Synechocystis* sp. PCC 6803 with the L subunit of photosynthetic bacterial reaction center of *Rb. sphaeroides* (SL) and *Rps. viridis* (VL). The D1 sequence is in lower case and the bacterial L sequences are in upper case.

```
SM *1   *AEYQNIFSQV*11 *QVRGPADLGM*21 *TEDVNLANRS*31 *GVGPFSTLLG
VM *1   *ADYQTIYTQI*11 *QARGPHITVS*21 *GEWGDNDRV-*30 *GKPPYSYWLG
D2                 *1  *          m*2  *tiavgrapv-*11 *egrwfdvldd

SM *41  *WFGNAQLGPI*51 *YLGSLGVLSL*61 *FSGLMWFFTI*71 *GIWFWYQAGW
VM *40  *KIGDAQIGPI*50 *YLGASGIAAF*60 *AFGSTAILII*70 *LFNMAAEVHF
D2 *21  *wl-krdrf-v*29 *figwsglllf*39 *pcafmalggw*49 *ltgttfvtsw

SM *81  *--NPAV--FL*87 *RDLFFFSLE-*96 *-PPAPEYG--*103*LSF---AAP-
VM *80  *--DPLQ--FF*86 *RQFFWLGLY-*95 *-PPKAQYG--*102*MGI---P-P-
D2 *59  *ythglassyl*69 *eganfltvav*79 *sspadafghs*89 *llflwgpeaq

SM *109*------LKEG*113*GLWLIASFFM*123*FVAVWSWWGR*133*TYLRAQALGM
VM *107*------LHDG*111*GWWLMAGLFM*121*TLSLGSWWIR*131*VYSRARALGL
D2 *99  *gnltrwfqig*109*glwpfvalhg*119*afgligfmlr*129*qfeisrlvgi

SM *143*GKHTAWAFLS*153*AIWLWMVLGF*163*IRPILMGSWS*173*EAVPYGIFSH
VM *141*GTHIAWNFAA*151*AIFFVLCIGC*161*IHPTLVGSWS*171*EGVPFGIWPH
D2 *139*rpynaiafsg*149*piavfvsvfl*159*myplgqsswf*169*fapsfgvagi

SM *183*LDWTNNFSLV*193*HGNLFYNPFH*203*GLSIAFLYGS*213*ALLFAMHGAT
VM *181*IDWLTAFSIR*191*YGNFYYCPWH*211*GFSIGFAYGC*221*GLLFAAHGAT
D2 *179*frfilflqgf*189*h-nwtlnpfh*198*mmgvagilgg*208*allcaihgat

SM *223*ILAVSR----*229*----FGGERE*235*LEQIADRGT-*244*AAERAALFWR
VM *231*ILAVAR----*227*----FGGDRE*233*IEQITDRGT-*242*AVERAALFWR
D2 *216*ventlfedge*228*dsntf---ra*235*feptqaeety*245*smvtanrfws

SM *254*--WTMGFNAT*262*MEGIHRWAIW*272*MAVLVTLTGG*282*IGIL-LS---
VM *252*--WTIGFNAT*260*IESVHRWGWF*270*FSLMVMVSAS*280*VGIL-LT---
D2 *255*qifgiaf-sn*264*krwlhffmlf*274*vpvtglwmss*284*vgivglalnl

SM *288*-G-TVV----*292*----D-NWYV*297*WGQNHGMA--*306*P
VM *286*-G-TFV----*290*----D-NWYL*295*WCVKHGAA--*303*P--------D
D2 *294*raydfvsqel*304*raaedpefet*314*fytknillne*324*gmrawmapqd

SM
VM *305*YP--AYL-PA*312*TPDPASLPGA*322*PK
D2 *334*qphenfifpe*344*evlprgnal
```

Fig. 2. Sequence alignment of D2 protein of *Synechocystis* sp. PCC 6803 with the M subunit of the photosynthetic bacterial reaction center of *Rb. sphaeroides* (SM) and *Rps. viridis* (VM). The D2 sequence is in lower case and the bacterial M sequences are in upper case.

General topology and evaluation of the model

The constructed PSII reaction center model, presented here, was refined using energy minimization methods in CHARMm (Brooks et al., 1983). At the end of the minimization, the energy of the model was $-33{,}350$ kcal/mol, compared to 2.39×10^{10} kcal/mol at the beginning of the minimization process (all measured with cofactors constrained). The general topology of the final PSII reaction center model resembles that of the bacterial reaction center (Fig. 3). The main-chain atoms of the constructed homology model deviate from their equivalent atoms in the *Rb. sphaeroides* reaction center by 0.818 Å RMS. Like its bacterial counterpart, the model has a twofold symmetry with an axis running from the center of the two chlorophylls of P680 to the non-heme iron. Both D1 and D2 proteins have five transmembrane α-helices in which cofactors responsible for the primary photochemistry are anchored. The transmembrane helices of D1 and D2 are denoted as A, B, C, D, E. The topology of 5 transmembrane helices for D1 and D2 is consistent with the evidence of the immunological assays (Sayre et al., 1986). There are also several short nonmembrane helices between the transmembrane helices on either the lumenal side or the stromal (cytoplasmic in cyanobacteria) side. These nonmembrane helices were based on the bacterial templates because the sequences are well conserved. No new secondary structures were introduced by the BLAST-searched protein fragments. In this model, there is very little β-sheet content that is in agreement with the Fourier transform infrared spectroscopy data (He et al., 1991). The detailed secondary structure profiles analyzed from the modeled D1 and D2 are shown in Figures 4 and 5, respectively. The definition for the boundaries of the transmembrane α-helices are slightly different from what was reported previously (Ruffle et al., 1992; Vermaas

Table 1. *Search results by the BLAST program through the Brookhaven Protein Data Bank for the unconserved loop sequences of Synechocystis sp. PCC 6803 D1 and D2 proteins*

Search query		Search results	
Protein and residue range	Sequence	Protein, PDB file code and residue range	Sequence
D1 (58–63)	VDIDGI	Aspartate aminotransferase, 3AAT (71–76)	LGIDGI
D1 (67–75)	VAGSLLYGN	Photosynthetic reaction center of *Rb. sphaeroides*, H-subunit, 4RCR.H (237–245)	VAGGLMYAA
D1 (225–231)	RETTEVE	Poliovirus, subunit 3, 2PLV.3 (226–232)	RDTTHIE
D1 (239–248)	FGQEEETYNI	Tryptophan synthase, Subunit B, 1WSY.B. (291–300)	DGQIEESYSI
D1 (294–298)	AFNLN	Tomato bushy stunt virus, Subunit A, 2TBV.A. (311–315)	TFNLS
D1 (303–309)	NQSILDS	Phosphoglucomutase, Subunit A, 2PMG.A. (39–45)	IQSIIST
D2 (98–104)	QGNLTRW	Cardio picornavirus coat protein, Subunit 1 2MEV.1 (139–145)	HGLLVRW
D2 (224–232)	EDGEDSNTF	Porin, 2POR (54–62)	ETGEDGTVF
D2 (300–307)	SQELRAAE	Apolipoprotein-E2, 1LE2 (57–64)	TQELRALM
D2 (325–332)	MRAWMAPQ	Methyltransferase, 3TMS (98–105)	WRAWPTPD

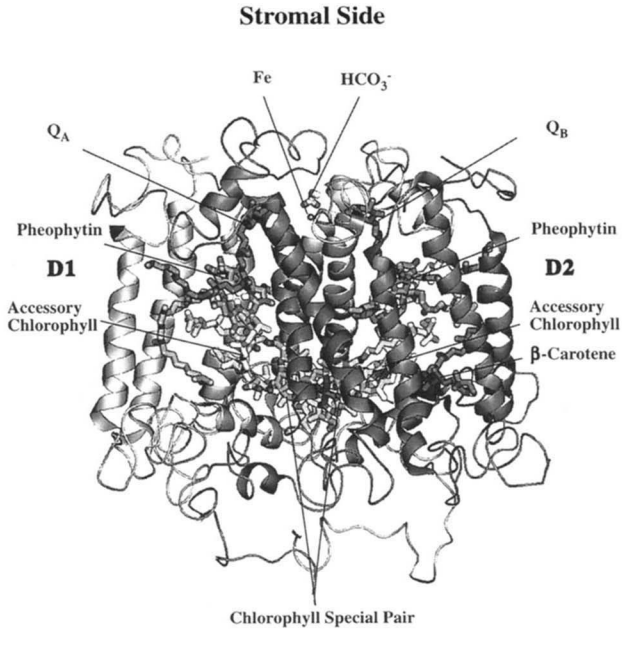

Fig. 3. Ribbon drawing diagram of the modeled three-dimensional structure of the PSII reaction center including cofactors. The ribbon form indicates the α-helix structure. D1 and D2 have five transmembrane helices each and several amphipathic helices in the lumenal and stromal (cytoplasmic in cyanobacteria) sides. The D1 protein is shown in light gray and D2 is shown in dark gray. Cofactors are represented in liquorice bond forms. Two bicarbonate anions were modeled in this structure, one in the non-heme iron site and the other in the Q_B binding niche (not shown as it is behind the D1 stromal [cytoplasmic] nonmembrane helix).

et al., 1993; Nixon & Diner, 1994; Svensson, 1995). The differences can be attributed to the different alignment and refinement procedures used in the modeling. The general profile of residue polarity was also examined: most of the charged or polar residues in the model are on the outside of the putative transmembrane spans and in the putative lumenal and stromal (cytoplasmic) sides, whereas the nonpolar and hydrophobic residues are in the putative membranous region, making the structure more stable.

The D1 and D2 interface is mostly composed of residues either in the transmembrane helices D and E or in the nontransmembrane regions (see e.g., Trebst, 1991). The contact residues between D1 and D2 are highlighted in Figures 4 and 5. The interactions between these contact residues are considered to play a key role in the assembly of the PSII reaction center and in maintaining a proper conformation of this protein complex. Mutations of some of these residues may result in complicated local and/or global effects, such as destabilization of the reaction center (Vermaas et al., 1987, 1990, 1994; Xiong et al., 1995; Hutchison et al., 1996), transduction of donor side mutational effect to the acceptor side (Roffey et al., 1994) or vice versa (Hutchison et al., 1996), and transduction of D2 mutational effects to D1 (Kless et al., 1993; Vermaas et al., 1994) or vice versa.

Our final PSII reaction center model was evaluated with the Protein Health subprogram in QUANTA. The D1 and D2 main-chain torsion angles were analyzed using the phi-psi plot (Ramachandran et al., 1963), which shows that 83.8% of the backbone conformations are within the most favored regions compared to 88.0% in the structure of *Rb. sphaeroides* L and M subunits. The quality of the model was also assessed using the newly developed probability density functions method (Subramaniam et al., 1996), which profiles the modeled structures against a standardized database of atom-pair probability density functions, including infor-

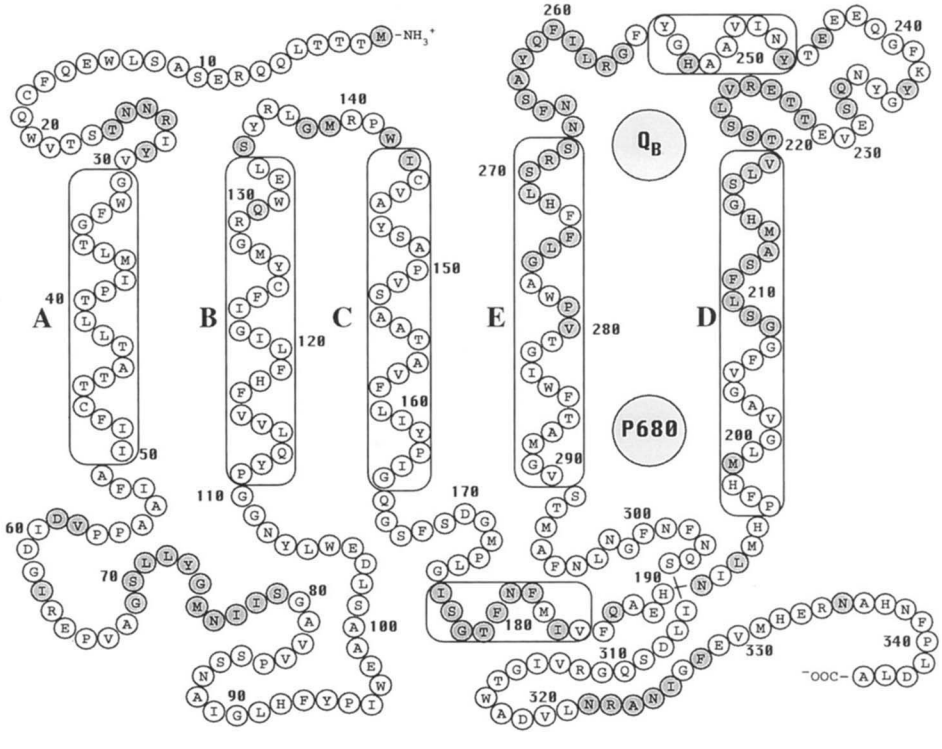

Fig. 4. Secondary structure profile of the modeled D1 protein. Predicted α-helical residues are boxed. Residues that are predicted to interact with D2 protein are highlighted. The stromal (cytoplasmic) side is on top, the lumenal side on the bottom.

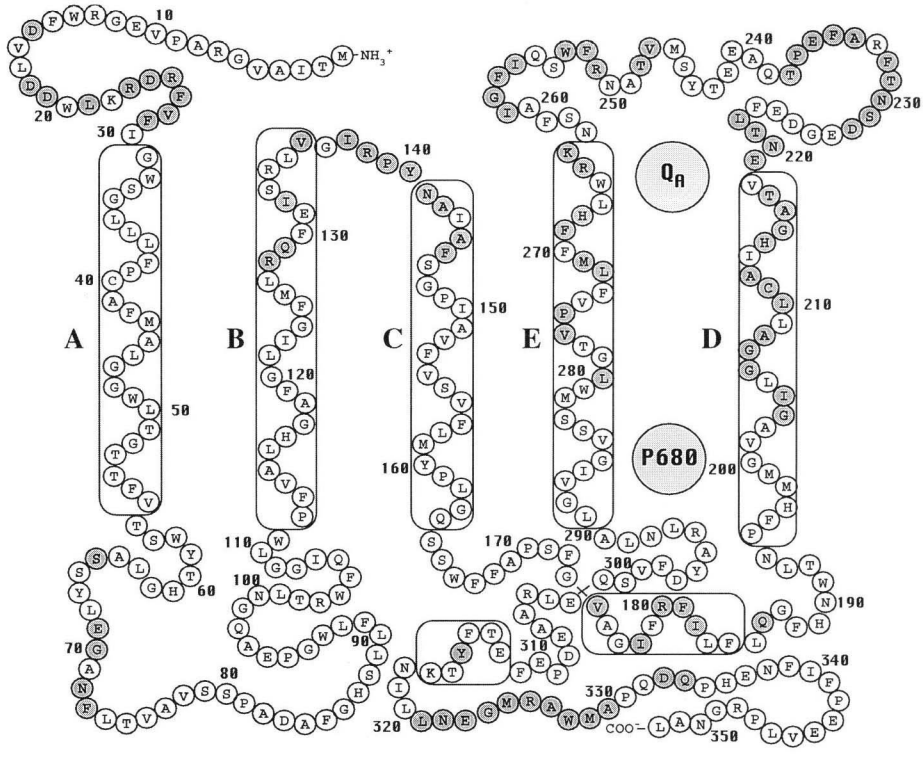

Fig. 5. Secondary structure profile of the modeled D2 protein. Predicted α-helical residues are boxed. Residues that are predicted to interact with D1 protein are highlighted. The stromal (cytoplasmic) side is on top, the lumenal side on the bottom.

mation on the distribution of distances between each pair of atoms in any pair of residues. The total number of atom types corresponding to the heavy atoms in the 20 amino acids is 167. The pairwise atomic distance PDFs are generated intraresidues, residues related by positions; n–n + 1, n–n + 2, and n–n + 3, and tertiary PDFs are computed separately for N to C and C to N terminal directions. The PDFs are assumed independent of each other. The total number of PDFs thus amount to 112,226 types and the number of atomic distance pairs in the 380 proteins considered are 80,670,588. Summary profiles at the atomic and residue level were generated for our modeled structure. In profiling, negative probabilities are unfavorable and probabilities above zero correspond to favorable contacts in resolution protein structures. The calculated results show that there are 0.0019% of highly improbable ($\log(P) < -9$) interatomic distances found in the model (440 of 22,535,541 interatomic distances measured), compared to 0.0016% of such improbable distances (250 of 15,193,828 interatomic distances measured) found in one of the templates used, the L and M subunits of *Rb. sphaeroides* reaction center. Thus, the comparison of PSII with bacterial reaction center is highly favorable.

Due to the varied sequence homology, different regions of the PSII reaction center model may have different levels of correctness. The transmembrane regions and the quinone-binding sites are highly conserved and have been modeled with a high degree of confidence. The stromal (cytoplasmic) and lumenal parts of the sequences, having many occurrences of insertions and deletions, can only be predicted with a relatively low degree of confidence. The conformation of the modeled C-terminal regions of both polypeptides, which are nonhomologous to the bacterial template and are, perhaps, in contact with other PSII subunits, are more speculative than other regions of the model.

General description of important cofactors

In this model, the cofactors essential for the PSII electron transfer include four chlorophylls, two pheophytins, one β-carotene, two plastoquinones, one non-heme iron, and two bicarbonate ions. Except for bicarbonate, other cofactors were modeled in the same location and the same geometric orientation as their counterparts in the bacterial reaction centers. Experimental evidence on the cofactor composition, P680 charge separation, and the electron transfer of PSII reaction center preparations supports the notion that the PSII chromophores are oriented similarly to those in the bacterial reaction center (Barber et al., 1987; van Dorssen et al., 1987; Shuvalov et al., 1989; Diner et al., 1991a). Quantitation of the PSII reaction center chromophores indicates that there are four to six chlorophylls, two pheophytins, and two plastoquinones (Nanba & Satoh, 1987; Gounaris et al., 1990; Kobayashi et al., 1990; van Leeuwen et al., 1991; Chang et al., 1994). Based on hole burning experiments, Chang et al. (1994) consider four chlorophylls to be the functionally limiting number in the PSII reaction center, making the pigment composition of PSII more homologous to that of the purple bacterial reaction centers.

Chlorophyll P680

There have been controversies concerning the number and orientation of the bound primary donor P680 chlorophylls in the PSII reaction center. On the basis of optical absorption difference measurements, van der Vos et al. (1992) proposed that P680 is a

monomer chlorophyll. However, an electron nuclear double resonance study by Nugent et al. (1994) showed that the $P680^+$ radical involves two weakly interacting chlorophylls. EPR studies showed that the ground state P680 is a dimer (Nugent et al., 1994). The measurement by Kwa et al. (1994) also ruled out the simple monomer model and suggested that P680 is most likely a dimer, but did not rule out the possibility of more than two excitonically coupled chlorophylls. Schelvis et al. (1994) suggested that P680 is a dimer asymmetrically oriented in the PSII reaction center. Thus, the majority of the studies appear to indicate that P680 is a dimer, at least in the singlet excited state. However, there are other suggestions as well. Vermaas (1993) suggested that P680 may consist of three chlorophylls (two homologous to the bacterial special pair and one to an accessory bacteriochlorophyll) that are in sufficient proximity that the positive charge and the triplet state are delocalized over the three molecules. Recently, Durrant et al. (1995) proposed that P680 should not be considered a strongly coupled dimer, but rather a weakly coupled multimer including the pheophytin electron acceptor. The final resolution of these possibilities will be available only from a high-resolution crystal structure of the PSII reaction center.

The orientation measurements of a light-induced spin-polarized chlorophyll triplet by van Mieghem et al. (1991) led to the conclusion that, in the PSII reaction centers, the ring of the triplet chlorophyll is at a 30° angle relative to the membrane plane, in contrast to the primary donor in the purple bacterial reaction center where they are essentially perpendicular to the membrane plane. It was suggested that this chlorophyll, which is P680, may resemble in geometry one of the accessory bacteriochlorophylls. Similar results were obtained by Bosch et al. (1995), who proposed a structural model of P680 based on the magnetophotoselection measurement of the triplet state P680, in which P680 is an excitonically-coupled dimer of chlorophyll *a*. Their model shows that two chlorophyll components of P680 are separated by 11 Å (center to center) and make an angle of 60°. The model of Svensson et al. (1995b), based on optical spectroscopic data, indicates that the dimeric P680 chlorophylls, which are oriented symmetrically and parallel to each other, are separated by 10 Å and the angle between the excitonic transition moments (Q_y) is 150°.

In view of the existing experimental suggestions, we propose here several possible alternative conformations for the chlorophyll P680 (Fig. 6). In the first model (Fig. 6A), we assume the arrangement of the special pair chlorophyll based on the bacterial counterpart to be valid. In this model, the two monomers of the P680 chlorophyll dimer are parallel to each other and perpendicular to the membrane plane. The magnesium ions in the center of the chlorophyll special pair are separated by 8.4 Å. The center-to-center distance of the primary donor is larger than that in the *Rps. viridis* reaction center, which may allow a more even distribution of exciton interactions between all pigments in PSII. The P680 model of Svensson et al. (1995b) and Svensson (1995), in which the special pair chlorophyll is also perpendicular to the membrane plane, has an even larger separation between the two monomers (10.1 Å).

In the P680 chlorophylls, the magnesium ions at the center of the P680 monomers are liganded by the specific histidine residues, D1-H198 and D2-H197, which, according to sequence comparison, match well with L-H173 and M-H210 (*Rps. viridis* numbering) of the bacterial special pair ligands. The ϵ2-nitrogen atoms of D1-H198 and D2-H197 are modeled 2.4 Å and 2.3 Å away from the coordinating magnesium, respectively. These two histidine residues are conserved in all known D1 and D2 sequences throughout the plants, algae, and cyanobacteria. Mutations made at these two histidine residues either lead to the loss of the PSII reaction center (see Vermaas et al., 1988; Nixon et al., 1992), or show a shift of 20–30 mV in midpoint potentials for $P680^+$/P680, thus supporting the role of these histidines in coordinating P680 (unpubl. data, cited in Vermaas, 1993).

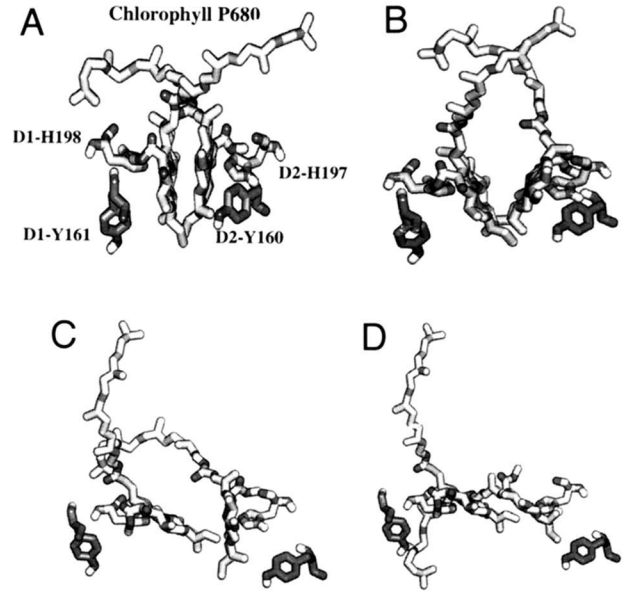

Fig. 6. Various possible models for the structures of P680 chlorophylls. The two histidines (D1-H198 and D2-H197) that ligand the magnesium in the center of the chlorophylls and the two redox active residues D1-Y161 (Z) and D2-Y160 (D) as electron donors to P680 are also shown. **A:** Possible conformation of P680 based on homology. The P680 chlorophyll dimer, which is assumed to be homologous to the bacteriochlorophyll special pair, has two monomers parallel to each other and perpendicular to the membrane plane that are separated by 8.4 Å. **B:** Possible conformation of P680 dimer based on the suggestion of Bosch et al. (1995). The two chlorophylls of the special pair are modeled to be distanced by 10 Å and to make an angle of ~60° (~30° with the vertical membrane axis). **C:** Possible conformation of P680 dimer based on the suggestion of Noguchi et al. (1993). The two chlorophylls of the special pair are arranged asymmetrically, with one of the chlorophylls perpendicular with the membrane plane and the other tilted by 30° relative to the membrane plane. They are separated by 8.4 Å. **D:** Possible conformation of P680 dimer based on the suggestion of Schelvis et al. (1994). The two chlorophylls are parallel to each other and make a 30° angle to the membrane plane and are separated by 8.4 Å.

Most of the residues lining the binding pocket for the P680 chlorophyll pair are hydrophobic and nonpolar. The P680 chlorophyll on the D2 side appears to be stacked by an aromatic residue, D2-W191. The closest modeled distance between the residue and the chlorophyll is 3.4 Å. Similar interaction was also suggested by Svensson (1995). No such ring stacking is observed for the P680 on the D1 side. Svensson (1995) suggested that the above tryptophan residue may also form a hydrogen bond to the ester group on the ring IV of D2 P680 chlorophyll. This hydrogen bonding was not observed in our model because the modeled distance is 8.6 Å. Svensson (1995) also suggested that residues D1-T286 and D2-S283 hydrogen bond to the ester groups on the ring IV of P680 on both the D1 and D2 sides. However, this was not supported in our model either. D1-M183 is positioned on the opposite side of the liganding D1-H198 and was suggested to have an electrostatic

interaction with the magnesium ion and one of the nitrogens of D1 P680 by Svensson (1995). We consider such interaction unlikely because the modeled distances between the sulfur atom and the above two atoms are 5.5 and 5.8 Å, respectively, in our model. We consider the possibility that the residue may form a van der Waals interaction instead with the chlorophyll because the methyl group is modeled to be 3.1 Å away from the chlorophyll.

Alternative structural models for the P680 special pair are proposed or reproposed here to account for existing experimental data in the literature. One such possible conformation of the chlorophyll P680 based on the suggestion of Bosch et al. (1995) results in a symmetrical structure for the two chlorophyll components. In this model (Fig. 6B), the two chlorophylls were separated by 10 Å, which make an angle of ~60° with each other. Each chlorophyll in the model has a ~60° angle relative to the membrane plane. This model matches the experimentally measured distance of 10.5 Å and an angle of 60° (Bosch et al., 1995).

According to a Fourier transform infrared spectroscopic study, which indicates the existence of an asymmetric dimer of chlorophyll *a* in the triplet state (Noguchi et al., 1993), an asymmetric P680 model was proposed (see review by Diner & Babcock, 1996). This conformation of P680 dimer suggests that one of the chlorophyll monomers is perpendicular to the membrane plane and the other tilted by 30° relative to the membrane plane. We have provided such a model with the two asymmetric chlorophylls (Fig. 6C). The distance between the centers of the two chlorophylls in the model is 8.4 Å.

Another possible conformation of P680 dimer that seems to account for more experimental data was proposed by Schelvis et al. (1994) (see Diner & Babcock, 1996). This suggestion implies that the two chlorophyll monomers are still parallel to each other but both are tilted by a 30° angle relative to the membrane plane. Thus, another alternative model for P680 is presented here (Fig. 6D). The modeled distance between the two chlorophylls is 8.4 Å, which is greater than that between the two monomers of the bacterial special pairs, as suggested by Diner and Babcock (1996).

The latter three alternative conformations (Fig. 6B,C,D) introduced enormous structural constraints to the protein part of the model, which was constructed based on homology. We thus modeled these chlorophylls separately from our main protein model. These models are only considered speculative suggestions for motivating further experimental verification. Currently, we favor the P680 model that was based on analogy with the bacterial primary donor (Fig. 6A), because it is the most energetically favorable conformation in our PSII reaction center model. In particular, the similar model of Svensson et al. (1995b) indicates that when the two P680 monomers that are perpendicular to the membrane plane are more than 10 Å away from each other, the conformation can be made to fit all existing experimental data.

Accessory chlorophylls

Our modeling of the two accessory chlorophylls that are not involved directly in primary charge separation is based strictly on their bacterial counterparts. The protein-binding environment of the accessory chlorophylls appears to be somewhat different from the ones in the bacterial reaction center if the chlorophylls occupy the same spatial position in PSII. The histidine residues that are coordinated with the magnesium ions in the bacteriochlorophylls (L-H153 and M-H180) are not conserved in D1 and D2. In our model, the residues close to the center of the two accessory chlorophylls are D1-T179 and D2-I178, which are modeled 3.9 Å and 4.2 Å to the magnesium, respectively. However, these two residues do not appear to be able to provide ligands to the respective magnesium ions as noticed previously in the pea model of Ruffle et al. (1992). Svensson (1995) proposed a possibility of water molecules acting as ligands for the chlorophylls. Aromatic residues D1-F180 and D2-F179 are found to be close (3.7 Å) to one of the pyrrole rings of the chlorophylls on either side, and it is expected that they may provide important ring-stacking interactions to the chlorophylls. Residue D2-L205 is in between the accessory chlorophyll and the active pheophytin on the Q_A side and is thought to serve as a conduit for electron transport, as noted in Ruffle et al. (1992).

Experimental models of accessory chlorophylls also exist. Based on the results from polarized fluorescence spectroscopy that the average orientations of the PSII chlorophylls are markedly different from those of the bacterial accessory chlorophylls, van Gorkom and Schelvis (1993) argued that a close association of the accessory chlorophylls with the P680 dimer is unlikely, and suggested that they should be separated by ~23 Å to allow an effective antenna function while minimizing the photo-oxidation process. Schelvis et al. (1994) postulated further that D1-H118 and D2-H117 may be the likely candidates for liganding the accessory chlorophylls. These two histidine residues in our PSII reaction center model are separated from the nearest accessory chlorophylls by more than 10 Å and thus a noncovalent interaction is considered unlikely without introducing new chlorophylls onto these two ligands.

Pheophytins

Modeling of the two pheophytins is also based on a strict homology with the bacteriopheophytins, which are positioned in the center of the hydrophobic membrane-spanning region. The most prominent binding interactions to the "redox active" pheophytin on the Q_A side are the hydrogen bonds to the keto group of the pheophytin provided by D1-R27 and D1-Q130 (modeled bond distances 2.3 Å and 2.5 Å, respectively). In many other species, D1-130 residue is a glutamate instead. Ruffle et al. (1992) and Svensson (1995) have modeled similar hydrogen bonding interactions between the pheophytin and D1-E130 (but not the arginine) in pea and spinach. In *Synechocystis* sp. PCC 6803, D1-Q130E mutation caused the pheophytin difference absorption spectrum to shift to the red by 3 nm (Giorgi et al., 1996), making it resemble the spectrum of the higher plants. It is suggested that in the higher plant system the glutamate may provide a stronger hydrogen bond to the pheophytin. In a related cyanobacterial species, *Synechococcus* sp. PCC 7942, there are two distinct forms of D1 protein, one (form I, encoded by *psbA*-1) having a lower photochemical yield and higher susceptibility to photoinhibitory damage than the other (form II, encoded by *psbA*-2 and -3) (Clarke et al., 1993; Kulkarni & Golden, 1994, 1995). The more efficient form II turns out to have a glutamate at 130 position, whereas the less efficient form I has a glutamine (see Svensson et al., 1991). Because this keto oxygen is part of the conjugated double bond system in the porphyrin, it is expected that a modified interaction at this position will have a considerable effect on the redox potential of the pheophytin (Svensson, 1995). Analogous situations were observed in purple bacteria; when mutations affected the hydrogen bonding pattern with bacteriochlorophylls, the redox potentials of the bacteriochlorophylls were changed (see, e.g., Wachtveitl et al., 1993).

In addition to the hydrogen bonding provided by D1-Q130, aromatic residue D1-Y147 is found to be close to one of the pyrrole rings and are thought to play a role in stabilizing the pheophytins. The side chain of D1-Y147 may also provide hydrogen bonding to the ester oxygen of the phytol branch (modeled distance 3.3 Å), consistent with the modeling result of Svensson (1995). The carbonyl group of the phytol branch of the same pheophytin probably forms a weak hydrogen bond with the hydroxyl group of D1-Y126, because the modeled distance between them is 3.4 Å. However, Svensson (1995) suggests that this tyrosine residue hydrogen bonds to the ester group on the ring IV of the pheophytin instead. An aromatic residue D2-W253 is found to be located between the Q_A head group and the "active" pheophytin and is separated from the porphyrin by 3.1 Å and from the Q_A by 3.7 Å. This residue has been suggested to be a "superexchange" mediator for the electron transport between pheophytin and plastoquinone (Plato et al., 1989). Another residue in between the same pheophytin and Q_A is D2-I213, which is positioned 4.5 Å from the porphyrin of pheophytin and 4.7 Å from the head group of Q_A, and may play a role similar to D2-W253.

In our model, the keto group on the ring V of the "inactive" pheophytin on the Q_B side is hydrogen bonded to D2-Q129 and D2-N142 (modeled bond distances from donor hydrogens to the hydrogen acceptors are 1.9 Å and 2.3 Å, respectively). The 2.3 Å bond may indicate either a weak H-bond or simply electrostatic interactions between the groups involved. The previous models (Ruffle et al., 1992; Svensson, 1995) had only the glutamine residue providing such hydrogen bonding interactions with the pheophytin. D2-F146 is modeled close to the ring IV of the pheophytin (3.1 Å) and its aromatic ring is also parallel to the pyrrole ring, allowing a ring-stacking interaction between them. The key hydrophobic residues located in between the "inactive" pheophytin and Q_B are D1-F255 and D1-M214, which are modeled to be 3.6 Å and 4.9 Å, respectively, away from the pheophytin, and 4.7 Å and 4.0 Å, respectively, from Q_B. The geometric orientation of D1-F255 is different compared to that of D2-W253. It is speculated that the distances and orientation of the two aromatic residues relative to the pheophytins may partially contribute to the unidirectional electron flow after the primary charge separation is over.

Supporting evidence for the above pheophytin modeling based on homology includes measurements on PSII chromophore stoichiometry (e.g., Chang et al., 1994) and the influence of site-directed mutagenesis on the pheophytin binding site on PSII electron transfer (see Diner & Babcock, 1996). However, the linear dichroism data that indicate oppositely signed LD features for pheophytins appear to argue against the strict analogy used above (Breton, 1990; van der Vos et al., 1992; van Gorkom & Schelvis, 1993).

β-Carotene

In the PSII reaction center model presented in this paper, we have also modeled one β-carotene molecule on the D2 side, by modifying the structure of dihydro-neurosporene from *Rps. viridis* (1PRC). This is the first effort in modeling of this chromophore in PSII. The carotenoid is located in the middle of the transmembrane region. The protein-binding environment for the carotenoid is exclusively hydrophobic, which includes D2-L45, D2-W48, D2-L49, D2-A71, D2-L74, D2-F91, D2-W111, D2-D112, D2-F113, D2-A115, D2-A119, D2-L116, D2-F153, D2-V154, D2-F157, D2-L158, D2-S172, D2-F173, D2-G174, D2-V175. The conformation of β-carotene is kinked with a conjugated π-system parallel to the membrane. The molecule was modeled to be within van der Waals contact with the accessory chlorophyll on the D2 side.

The carotenoid in the bacterial system is suggested to protect the reaction center against photo-oxidation by quenching the triplet state of the bacteriochlorophyll special pair (see review, Lancaster et al., 1995). Similarly, the function of β-carotene in the PSII reaction center is thought to be related to the protection of the PSII reaction center from damage by excess light through dissipation of excess excitation energy, as heat, on the special pair chlorophyll (Telfer et al., 1994). The close proximity of β-carotene to the accessory chlorophyll supports a high probability that it may function in quenching the triplet state of primary donor P680 via the accessory chlorophyll, analogous to the role of carotenoid in the bacterial reaction center.

Donors to $P680^+$

Oxygen evolution takes place in PSII only when the PSII reaction center is in association with several other PSII proteins (for reviews, see Ghanotakis & Yocum, 1990; Vermaas & Ikeuchi, 1991; Vermaas et al., 1993). The D1 and D2 residues at the lumenal side have high affinity for a manganese cluster (Coleman & Govindjee, 1987; Debus, 1992), which serves as a charge accumulator device during water oxidation (for reviews see Hansson & Wydrzynski, 1990; Diner et al., 1991a; Debus, 1992; Renger, 1993; Babcock, 1995). Site-directed mutagenesis studies on D1 and D2 have led to the identification of two redox active residues, D1-Y161 and D2-Y160, which are electron donors to chlorophyll $P680^+$. D1-Y161, or the donor Z (also called Y_Z), is a rapid electron donor to the $P680^+$ (Debus et al., 1988b; Metz et al., 1989); and the D2-Y160, or the donor D (also called Y_D), is a slow donor (Debus et al., 1988a; Vermaas et al., 1988).

The two tyrosine residues in the model were arranged symmetrically around the special pair chlorophylls and in relation to the non-heme iron. Both of the residues are positioned such that their hydroxyl groups are pointing toward the lumen. The spatial relationships of the residues with D1-H198 and D2-H197 that serve as ligands for the chlorophyll special pair are shown in Figure 6. The modeled distance from the D1-Y161 phenolic oxygen to the center of the nearest chlorophyll P680 monomer is 12.8 Å. This matches well with the experimentally determined distance of 10–15 Å (Hoganson & Babcock, 1989). The measured distance between D1-Y161 and D2-Y160 is 30.6 Å, which matches closely the experimentally measured 29–30-Å distance (Astashkin et al., 1994; Kodera et al., 1995). The modeled distances of the tyrosines Z and D to the non-heme iron are 36.5 Å and 34.2 Å, respectively, which fall in the range of the EPR spectroscopic measurements of 37 ± 5 Å by Hirsch and Brudvig (1993) and Koulougliotis et al. (1995). The EPR-estimated distance from donor D to the non-heme iron by Kodera et al. (1992) is 26–33 Å. The above experimental studies provide strong support for the validity of this PSII three-dimensional model.

The amino acid environment surrounding the two tyrosine residues may affect the functions of Z and D. In this model, the residues that are located between D1-Y161 and the nearest P680 chlorophyll are D1-A156, D1-F186, D1-A287, D1-M288, D1-G289, D1-V290, D1-S291, D1-T292, and D1-M293. Most of these residues may be crucial in mediating the electron transfer from the donor Z to $P680^+$. The modeled Z and D residues do not seem to hydrogen bond with the histidine residues that coordinate P680, as noted previously (Svensson et al., 1990). Other residues surround-

ing D1-Y161 within 5 Å are D1-T155, D1-V157, D1-F158, D1-L159, D1-I160, D1-P162, D1-I163, D1-G164, D1-Q165, D1-G166, D1-N298, D1-G299, D1-N301, D1-N303, and D1-Q304. The binding environment is somewhat hydrophilic for the donor Z. Some of the residues, such as D1-S167, were suggested to provide ligands to the manganese cluster (Ruffle et al., 1992). Site-directed mutagenesis of D1-H190 in *Chlamydomonas reinhardtii* indicates that this residue may be involved in assembly of the manganese cluster (Roffey et al., 1994). D1-H190 was suggested to be in close vicinity to donor Z (4 Å) by Svensson (1995) and an electrostatic interaction between the two residues was proposed. However, this is not in agreement with our current model, because the respective distance from the tyrosine to the histidine is 9.0 Å. Mutation of this residue to a phenylalanine resulted in a spectrum very similar to the wild-type, suggesting that the histidine may not be in such a close contact with the donor Z (Kramer et al., 1994; Roffey et al., 1994). Mutations on D1-H195 were shown to have lowered oxygen evolution and a shifted equilibrium constant between Tyr_ZP680^+ and $Tyr_Z^{ox}P680$, most likely due to a change in the midpoint potential for Tyr_Z/Tyr_Z^{ox} couple (Kramer et al., 1994; Roffey et al., 1994). This residue was modeled to be off the contact distance from either Z or P680. However, it is positioned 3.1 Å from D1-M293, which is also 3.1 Å from Z. Thus, impacts of indirect structural changes in the binding environment for the donor Z may be attributed to its slowed electron transfer to P680.

Manganese cluster, which is crucial in water oxidation and reduction of the donor Z, was not included in this model. An aspartate residue, D1-D170, was implicated experimentally in binding to the Mn cluster at the PSII donor side (Nixon & Diner, 1992; Chu et al., 1995). The distance between the manganese cluster and the donor Z measured by the electron spin echo ENDOR experiments was shown to be 4.5 Å (Gilchrist et al., 1995). It is conceivable that one of the manganese ligands, D1-D170, should be located in close proximity to the donor Z, as presented in Svensson (1995). In our PSII reaction center model, this aspartate residue was modeled at slightly more than the van der Waals contact distance (6.4 Å), which is somewhat in agreement with the previous experimental and theoretical studies. However, another acidic residue, D1-E189, which was also suggested to be close to D1-Y161 (Svensson, 1995), is not observed in our model because the interresidue distance is 12.2 Å.

The model of Svensson (1995) suggests that D2-H190 (higher plant numbering) is hydrogen bonded to the donor D, because the distance between the ϵ2-nitrogen of D2-H190 and the phenolic oxygen of D2-Y160 is 2.8 Å. This is not in agreement with our model because the corresponding distance in our model is 7.9 Å. D2-Q164 was proposed to hydrogen bond to the donor D in Svensson (1995); this also is inconsistent with our model because the corresponding distance is 6.2 Å. Instead, the phenolic oxygen of the donor D appears to hydrogen bond to the main-chain oxygen of D2-F169 (the modeled distance is 2.8 Å).

Diner et al. (1991a) suggested that some of the D1 C-terminal residues (D1-H332, D1-D342, D1-A344) are involved in the assembly of the oxygen-evolving complex and in manganese binding. However, these residues are found at a long distance (more than 27 Å) from the donor Z in this model. It is not clear to us how their role can be exerted at such a distance. It may be possible that the C-terminus is folded under the transmembrane helices, as suggested by Nugent et al. (1994). However, without further experimental evidence to direct the modeling, we have to leave this question open. Because oxygen evolution is unique in PSII and the primary structures of D1 and D2 tend to have low homology with the bacterial reaction center in the C-terminal region, accurate modeling of the oxygen-evolving complex may be difficult at this stage.

Plastoquinone Q_A and its binding niche

The primary plastoquinone Q_A, a bound one-electron carrier, was modeled in the region between helices D and E of D2, although the rest of the transmembrane regions on the "active" side are dominated by the D1 protein. The D2 residues that provide specific interactions to Q_A include D2-T217, D2-N230, D2-S262 and D2-N263; they may contribute to the Q_A binding by providing hydrogen bonds to the carbonyl oxygen of Q_A. One of the Q_A carbonyl oxygen atoms can form a weak bifurcal hydrogen bond to the side-chain hydroxyl group of D2-T217 and the amide group of D2-N230. The modeled bond distances are 2.8 and 2.3 Å (from donor hydrogens to the acceptor oxygen), respectively. Another Q_A carbonyl oxygen may also hydrogen bond to more than one residue donor atoms. The main-chain amide hydrogens of D2-S262 and D2-N263 are both possible donors for the hydrogen bonds because the modeled distances from the Q_A oxygen atom to the hydrogen donors of D2-S262 and D2-N263 are 2.4 and 2.8 Å, respectively. Among the residues that form a tight binding niche, those that are considered to be involved in interacting with the head group of Q_A are mostly polar or positively charged. They are D2-H214, D2-T217, D2-T221, D2-N230, D2-A249, D2-N250, D2-W253, D2-S254, D2-S262, D2-N263, D2-K264, D2-L267. Those residues that are considered to be more likely to interact with the isoprenoid chain of Q_A are mostly hydrophobic. They are D2-L209, D2-L210, D2-I213, D2-Q255, D2-I259, D2-A260, D2-F261, and D2-W266. As mentioned previously, D2-W253 is a critical residue that may function in mediating the electron transfer between pheophytin and Q_A. In addition, the ring system of D2-W252 is parallel to Q_A and thus may allow the residue to stack with Q_A and stabilize Q_A binding.

An electron spin echo envelope modulation experiment suggested hydrogen bonding between Q_A^- and a histidine residue (Astashkin et al., 1995). If this bonding pattern indeed exists, we consider D2-H214 to be a likely candidate to provide such a bonding because its δ1-hydrogen is modeled to be 3.5 Å away from one of the Q_A carbonyl oxygens. However, the isotopic labeling experiment of Tang et al. (1995) did not confirm the coupling of a histidine nitrogen with Q_A^-.

Plastoquinone Q_B and its binding niche

The secondary plastoquinone Q_B is a two-electron carrier and can be doubly reduced by Q_A^-. The Q_B binding niche has long been the subject of intensive research because this binding site is also the site for herbicide binding (see reviews, Oettmeier, 1992; Vermaas, 1993).

The Q_B binding niche is formed predominantly by D1 residues that fall between the helices D and E of the D1 protein. Interestingly, there are also a number of D2 residues that are identified to be in the Q_B niche (also see Trebst, 1991). The residues that are modeled to provide hydrogen bonding to the carbonyl oxygen atoms of Q_B are D1-H215, D1-H252, and D1-S264. The modeled hydrogen bond distances between one of the Q_B oxygens and the hydrogen donors of D1-H252 and D1-S264 are 3.1 Å and 2.8 Å, respectively. The other Q_B oxygen is hydrogen bonded to D1-

H215 at a bond distance of 2.3 Å (a weak bond). D1 residues identified to be more likely related to the binding of the head group of Q_B are D1-H215, D1-V219, D1-Y246, D1-A251, D1-H252, D1-F255, D1-S264, D1-N266, and D1-L271. A D2 residue D2-F232 is found in close association with the Q_B head group. The residues that are identified as responsible for interacting with the isoprene tail also involve both D1 and D2 proteins. They are D1-F211, D1-M214, D1-I259, D1-F260, D1-Y262, D1-A263, D1-F265, D2-I30, D2-L37, D2-F38, D2-F125, D2-R128.

Mutational studies on D1-S264 and D1-H252 have implicated their close association with Q_B. Taoka and Crofts (1990) show that D1-S264G mutation raises the dissociation constant (K_q) of Q_B by a factor of 10, although it has little effect on the forward rate constant that is related to the Q_B protonation. The bacterial homologue of D1-S264, L-S233 (*Rps. viridis* numbering), has been suggested to play a role in stabilizing the Q_B protonation intermediate, Q_BH^- (Lancaster & Michel, 1996). It is not yet known whether D1-S264 may assume a similar role in PSII. Mutations of D1-H252 to leucine or glycine have been shown to lower the apparent equilibrium constant (K'_{AB}) by a factor of 10 for the reaction $Q_A^- + PQ + Q_AQ_B = Q_AQ_B^-$ (Diner et al., 1991a, 1991b; Nixon et al., 1992). More detailed discussion on the role of D1-H252 in the Q_B protonation will be presented in a later section. D1-F255 may also be a critical residue in Q_B binding, as is its bacterial counterpart, L-F216, in the refined model of Lancaster et al. (1995), where the phenyl ring of L-F216 appears to stack with the Q_B head group. Although the phenyl ring of D1-F255 in our model is not parallel to the aromatic ring of Q_B corresponding to the structure in the bacterial templates (1PRC and 2RCR), it is still modeled within van der Waals contact distance to Q_B (4.2 Å), which may support its role in providing strong hydrophobic interactions with the plastoquinone.

Herbicide DCMU binding

PSII herbicides are known to displace Q_B from its binding niche and to inhibit the electron transfer from Q_A to Q_B (Velthuys, 1981; Wraight, 1981). In our modeling, we used DCMU, one of the most commonly used phenylurea type of herbicides and modeled its position in the Q_B site.

Modeling of DCMU to the Q_B niche (Fig. 7) was based on the available crystal structure information of DCMU binding in a bacterial reaction center. DCMU that binds to PSII does not normally bind to the bacterial reaction center. However, analyses of *Rps. viridis* mutants showed that a mutation (L-Y222F) resulted in the reaction center being "PSII-like" by becoming receptive to urea type herbicides (e.g., DCMU) (Sinning et al., 1989). The X-ray structure of this mutant (T4) reaction center with bound DCMU is available (Sinning et al., 1990; Sinning, 1992). The structure shows that the mutation eliminates the hydrogen bonding between the L-Y222 and M-D43, causing a slight movement of a stretch of M residues that shield the Q_B site, thus widening the Q_B binding pocket. DCMU phenyl ring was turned by 180° compared with Q_B. In our modeling, we assumed that DCMU adopted a conformation similar to that in the bacterial reaction center. This assumption was supported by the evidence that DCMU binding to T4 resulted in similar semiquinone-EPR signals to that in PSII (Sinning et al., 1989). Following the insertion of DCMU protein-binding environment surrounding the herbicide was refined through energy minimization and molecular dynamics simulations. The

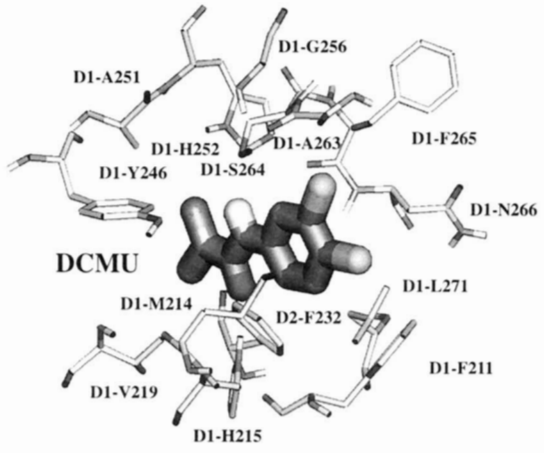

Fig. 7. Herbicide DCMU modeled in the Q_B binding niche according to its binding pattern determined in the crystal structure of a mutant *Rps. viridis* reaction center. The protein binding environment for DCMU is shown. The side chain of D1-H215 is predicted to provide hydrogen bonding to the carboxyl oxygen of DCMU. D1-S264 may provide a hydrogen bond with the amide group of DCMU.

final CHARMm energy of the DCMU binding niche is −1,200.5 kcal/mol compared to 95,969.7 kcal/mol before minimization.

The protein binding environment for DCMU is found to be overlapping with that for Q_B, although not identical. The residues that appear to coordinate the herbicide binding are D1-F211, D1-M214, D1-H215, D1-V219, D1-F232, D1-Y246, D1-A251, D1-H252, D1-G256, D1-A263, D1-S264, D1-F265, D1-N266, and D1-L271, as shown in Figure 7. D1-H215 δ1-hydrogen is likely to provide a weak hydrogen bond to the carbonyl group of DCMU with the modeled bond distance at 2.3 Å. D1-H215 is homologous to L-H190 in bacterial reaction center, which was also found to hydrogen bond to DCMU in the T4 mutant reaction center (Sinning, 1992). D1-S264 may provide another hydrogen bond through its hydroxyl oxygen to the amide hydrogen of DCMU. The modeled bond distance is 2.7 Å. We consider that the herbicide may also hydrogen bond with the amino acid residues via water molecules, as is the case in triazine binding to the bacterial reaction centers (Lancaster et al., 1995).

Numerous studies have been conducted on site-specific mutations in the Q_B niche that induce modified binding specificities for DCMU (for review see Oettmeier, 1992). Well-known single mutations that have caused DCMU resistance, such as D1-F211S, D1-V219I, D1-G256D, D1-A251V, and D1-S264A, can all be explained by our constructed model because these residues are found within the van der Waals contact sphere with DCMU (Fig. 7). The herbicide resistance mutations may thus be due to the modified van der Waals or electrostatic interactions of DCMU with its protein binding environment.

Non-heme iron and the liganding histidines and bicarbonate

In the bacterial reaction center, the non-heme iron is coordinated by six ligands, one from each of the four histidines (L-H190, L-H230, M-H227, M-H264) and two from a glutamate (M-E232, *Rps. viridis* numbering) (cf. Michel & Deisenhofer, 1988). The four histidines are conserved in all known D1/D2 sequences. The involvement of histidine ligation in PSII is supported by the extended X-ray absorption fine structure spectroscopic studies (Bun-

ker et al., 1982). However, the M-E232 residue is not conserved in the D1/D2 polypeptides. Michel and Deisenhofer (1988) and van Rensen et al. (1988) proposed that bicarbonate could serve as a functional homologue of M-E232 in PSII. The possible role of bicarbonate liganding with the non-heme iron was further supported by EPR and Mössbauer measurements (Diner & Petrouleas, 1990; Petrouleas & Diner, 1990).

In our PSII reaction center model, as in the bacterial template, the four histidine residues, D1-H215, D1-H272, D2-H214, and D2-H268, ligand with the non-heme iron (Fig. 8). Their ϵ2-nitrogens are liganded to the non-heme iron and the modeled bond distances are from 1.9 to 2.0 Å. Mutation on D2-H268, changing it to glutamine (Vermaas et al., 1994), caused the mutant to lose the autotrophic growth and result in a total inhibition of electron transport from Q_A^- to the plastoquinone pool. Both Q_A and Q_B niches were shown to be perturbed significantly in the mutant, which could be explained by the loss of the non-heme iron. Because this mutation also caused destabilization of the PSII assembly, part of the phenotypic effect can also be attributed to the residue being at the interface of D1 and D2 (see above). Mutations on D2-H214 and nearby residue D2-G215 also resulted in destabilization of the PSII reaction center and disturbed local structure around Q_A and the non-heme iron (Vermaas et al., 1987, 1990). The above experimental evidence supports the ligation of the non-heme iron to the histidine residues.

In our refined PSII reaction center model, no D1 or D2 glutamate residue appears to substitute the bacterial M-E232. Therefore, to satisfy the iron-liganding requirement, a bicarbonate ion was docked to the iron center and allowed to assume the same position as the carboxyl group of M-E232 in the bacterial reaction center based on the available experimental and theoretical suggestions. The modeled distances between the carboxylic oxygens of the bicarbonate and the non-heme iron are modeled to be 2.7 and 3.2 Å, respectively. Thus, the bicarbonate appears to provide the fifth and the sixth ligand to the non-heme iron. In contrast, in the pea PSII model (Ruffle et al., 1992), D1-E231 was modeled to assume the structural homologue of M-E232 from the bacterial reaction center and appears to provide two ligands to the iron. In the absence of a final crystal structure, this possibility can be tested using site-directed mutagenesis.

The direct involvement of bicarbonate in binding to the iron is supported by several lines of evidence. Vermaas and Rutherford (1984) found that formate treatment to thylakoid membranes increases the Q_A^--Fe^{2+} EPR signal ($g = 1.82$) by 10-fold. Mössbauer spectrum of Fe signal, indicative of the inner-coordination sphere of iron, was found to be affected significantly by the addition of formate and the signal was restored upon the readdition of bicarbonate (Diner & Petrouleas, 1987; Semin et al., 1990). NO has been shown to be able to ligand to the non-heme iron of PSII and to exhibit a characteristic Fe^{2+}-NO-EPR signal ($g = 4$). Addition of bicarbonate is able to suppress the Fe^{2+}-NO-EPR signal (Petrouleas & Diner, 1990). A recent Fourier transform infrared difference spectroscopy study using ^{13}C-labeled bicarbonate has further indicated that bicarbonate is a bidentate ligand of the non-heme iron in PSII (Hienerwadel & Berthomieu, 1995). All these experiments strongly suggest that bicarbonate is able to compete with formate or NO for ligation with the non-heme iron.

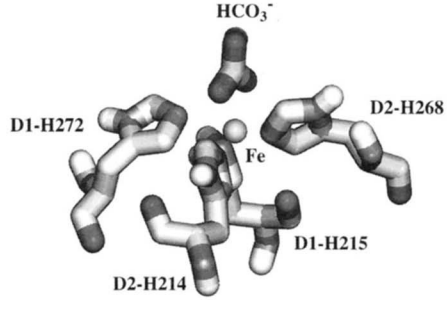

Fig. 8. The non-heme iron of the modeled PSII reaction center shown to be coordinated by four histidines, D1-H215, D1-H272, D2-H214, D2-H268, and a bicarbonate (HCO_3^-). The bicarbonate anion was modeled to provide a bidentate ligand to the iron.

In our model, two residues from D1 and D2, D1-V219 and D2-F232, may also form a part of the close binding niche (5 Å sphere) for the non-heme iron. This binding pocket is similar to that in the bacterial reaction center, where L-I194 and M-I223 occupy similar spatial positions and participate in forming the binding pocket for the iron. The partial PSII model of Svensson (1995) indicates that D1-S268 and D2-K265 (higher plant numbering) form hydrogen bonds with the ϵ2-hydrogens of D1-H272 and D2-H268, respectively. However, this is not supported in our model because the corresponding distances are 4.9 Å and 3.8 Å, respectively.

In our PSII model containing the bicarbonate, the residues that seem to form a binding pocket for the bicarbonate are positively charged and hydrophobic, which include D1-L233, D1-V219, D2-N230, D2-T231, D2-F232, D2-R233, D2-A234, D2-P237, and D2-K264, in addition to the four iron-liganding histidines mentioned above. Among these residues, D2-R233 was shown to be involved in binding and/or stabilizing bicarbonate and formate in vivo (Cao et al., 1991). The hydroxyl oxygen of the bicarbonate is separated from the main-chain amide hydrogen of D2-R233 by 4.8 Å. However, D2-K264 appears to be the most likely candidate to interact directly with the bicarbonate anion; the modeled distance from one of the ζ hydrogens of the lysine to the closest carbonyl oxygen of bicarbonate is 3.9 Å. Involvement of D2-K264 for binding with the bicarbonate has been confirmed by Diner et al. (1991b).

An in vivo role of bicarbonate binding to the non-heme iron has been postulated (Govindjee & van Rensen, 1993). The bound bicarbonate, in addition to effects on the donor side of PSII (El-Shintinawy & Govindjee, 1990; Klimov et al., 1995), may serve to stabilize the Q_A-Fe-Q_B structure; and upon the removal of bicarbonate, the distance between Q_A and Q_B may be altered, slowing the electron transfer rate, although a larger effect is in the protonation of reduced Q_B.

We speculate here that there may be a channel within the PSII complex that leads to the iron center from the outside environment. The channel may be just small enough to allow small molecules or ions such as water or bicarbonate to pass through. If such a channel exists, certain positively charged residues in both D1 and D2 may serve to increase the affinity of bicarbonate. Within 20-Å distance to the bicarbonate modeled in our PSII reaction center, several positively charged residues are identified. They are D1-R27, D1-R225, D1-R140, D1-R225, D1-K238, D1-H252, D1-R257, D1-R269, D2-K23, D2-R24, D2-R26, D2-R239, D2-R233, D2-R251, D2-K264, and D2-R265. As discussed below, some of these residues, such as D1-R269, D2-R233, D2-R251, D2-K264, and D2-R265, have been shown to have dramatic influence on the binding, stabilization, and functioning of bicarbonate in PSII (Cao et al.,

1991; Diner et al., 1991b; Xiong et al., 1995). It is likely that the physiological role of these residues may extend beyond the binding to bicarbonate. It may also be involved in PSII assembly.

D2-K264 is modeled 3.9 Å away from bicarbonate, suggesting its crucial role in bicarbonate binding to the iron center. Site-directed mutations at D2-K264 showed that the mutants have a reduced rate of electron flow from Q_A^- to Q_B and are very resistant to formate and NO treatment (unpubl. data, cited in Diner et al., 1991b). In addition, the D2-K264X mutants require much higher levels of bicarbonate to increase the electron flow from Q_A^- to Q_B, suggesting that the residue is involved in the binding of bicarbonate. The mutants of another nearby positive residue, D2-R265, showed a similar behavior, although to a lesser extent (Diner et al. 1991b). Two other positively charged residues on the D2 protein (D2-R233 and D2-R251, but not D2-R139) of cyanobacteria near the non-heme iron have been investigated for involvement in bicarbonate effect. Both have been shown to strongly affect the formate susceptibility of PSII and were suggested to stabilize the bicarbonate binding in vivo (Cao et al., 1991; Govindjee, 1993). Govindjee et al. (1991) showed that a herbicide-resistant mutant in *C. reinhardtii* D1-L275F fails to show the bicarbonate-reversible formate effect. This residue is located near the middle of transmembrane helix E and is not close to the iron-liganding bicarbonate (8.1 Å). However, it is separated from one non-heme iron ligand D2-H214 by 4.0 Å. It is speculated that this mutation perturbs the binding environment of the non-heme iron significantly, and thus the binding of bicarbonate. To investigate the involvement of D1 arginine residues in the bicarbonate binding, a D1 arginine nearest to the bicarbonate in the iron site, D1-R269, which is 8.5 Å away from the putative bicarbonate (α-carbon of D1-R269 to the hydroxyl oxygen of bicarbonate), was mutated to a glycine (Xiong et al., 1995; Hutchison et al., 1996; J. Xiong, R. Hutchison, R. Sayre, & Govindjee, submitted to *Biochim. Biophys. Acta*). The mutant appears to be ~4-fold less sensitive to formate inhibition than the wild type. EPR analysis of the mutant suggests that the putative iron-formate (a bicarbonate analogue) liganding still exists but is perturbed greatly, suggesting that D1-R269 may not be involved directly in binding the bicarbonate at the iron but may affect the conformation of the bicarbonate-iron center. We suggest that the general characteristics of the electrostatic field near the non-heme iron sometimes plays an important role in allowing the bicarbonate anion to diffuse to the site.

Bicarbonate in the Q_B niche

In addition to liganding to the iron, many experiments have suggested that bicarbonate may also function in promoting the protonation of Q_B^- or Q_B^{2-} (Eaton-Rye & Govindjee, 1988a, 1988b; van Rensen et al., 1988; Xu et al., 1991). Kinetic studies by Blubaugh and Govindjee (1988b) suggested the possibility of two high-affinity bicarbonate binding sites in the PSII reaction center. This second binding site is likely to exist in the Q_B niche and is considered to be related to the protonation of plastoquinone. Characterization of a number of Q_B mutants that are also herbicide resistant have implicated the Q_B binding niche to be involved for the bicarbonate functioning in PSII (Govindjee et al., 1990, 1992; Cao et al., 1992; Strasser et al., 1992; Mäenpää et al., 1995; Srivastava et al., 1995; Vernotte et al., 1995). The tested residues involved are: D1-F211, D1-V219, D1-E242, D1-E243, D1-E244, D1-A251, D1-F255, D1-G256, D1-S264, D1-N266, D1-L275. These residues and others near the non-heme iron mentioned above that affect the bicarbonate stabilization, binding, and functioning in the PSII reaction center are shown in Figure 9.

In the bacterial reaction centers, aspartate 213 and glutamate 212 on the L subunit are in close proximity to the ubiquinone and were shown to be important for Q_B protonation (see the review by Okamura & Feher, 1995). However, on the Q_B binding domain in D1, there are no carboxylate residues near the quinone head group. We consider it likely that there may be a bicarbonate anion in this site functioning as a homologue of an aspartate or a glutamate in the bacterial reaction center, shuttling protons between Q_B and external aqueous environment (see Blubaugh & Govindjee, 1988a; Govindjee & van Rensen, 1993).

Because bicarbonate is anionic, it is very likely that its binding at the Q_B niche would be electrostatic in nature and, therefore, positively charged amino acid residues in D1 are likely to participate in bicarbonate binding. In the 6-Å vicinity from Q_B, two histidines (D1-H215 and D1-H252) and only one arginine (D1-R257) are found. Because D1-H215 is modeled in the middle of the transmembrane helix D, providing ligands to the non-heme iron, it seems unlikely that it also serves the role of bicarbonate binding because this would be expected to perturb the liganding with the iron while bicarbonate undergoes the cycle of being deprotonated and protonated. Although we cannot rule out this possibility, we consider it more reasonable to assume that a bicarbonate may be located closer to D1-H252 and/or D1-R257. This suggestion is consistent with that of Blubaugh and Govindjee (1988a) in which D1-R257 binds a bicarbonate at the Q_B site, transferring protons between D1-R257 and D1-H252.

In the Q_B niche of our model, the carbonyl oxygens of Q_B appear to provide a bifurcated hydrogen bond with both D1-H252 and D1-S264. This is different from the model of Blubaugh and Govindjee (1988a), in which D1-H252 does not hydrogen bond with Q_B in its fully oxidized form. In that model, a bicarbonate was modeled in between D1-H252 and D1-R257 in an attempt to explain the Q_B protonation. The bicarbonate anion is stabilized by D1-R257 and provides a proton, through D1-H252 intermediate, to Q_B in both the singly and doubly reduced forms after each charge separation.

Because studies of the protonation of Q_B in the bacterial reaction centers (Wraight, 1979; Maróti & Wraight, 1988; McPherson et al., 1988) suggest that, when Q_B is in the semiquinone form

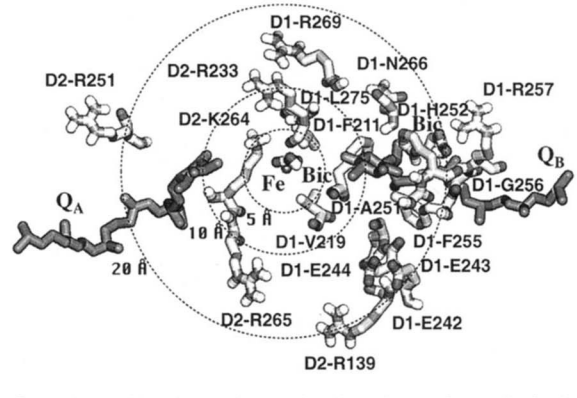

Fig. 9. Amino acid residues that are implicated experimentally in the bicarbonate stabilization, binding, and functioning in the acceptor side of the PSII reaction center. Concentric rings indicate the distances away from the non-heme iron.

(Q_B^-), it is not protonated but only partially neutralized by the protein environment of the reaction center and that Q_B is only protonated after it is doubly reduced, we modified the model of Blubaugh and Govindjee (1988a) and allowed the protonation to occur only after Q_B becomes Q_B^{2-}. In our current model, the bicarbonate is anchored in such a way that its hydroxyl group is hydrogen bonded to the δ1-nitrogen of D1-H252, whereas its carboxyl group is hydrogen bonded to the positively charged δ-guanido group of D1-R257 (Fig. 10A). In order to explain that Q_B is in fact stabilized by a positive charge in the binding environment, a water molecule that serves as a potential proton donor to D1-H252 is introduced in our model. This water molecule is docked near the ϵ2-nitrogen of the histidine while it is stabilized by a nearby D2-K23 through a hydrogen bond. This lysine on D2 does not appear to be able to bind a bicarbonate through electrostatic forces because its positive charge appears to be neutralized by a nearby aspartate, D2-D25.

Based on some earlier ideas of Blubaugh and Govindjee (1988a) and our refined three-dimensional PSII reaction center model, we propose a working hypothesis concerning the Q_B protonation (Fig. 10B). Our hypothesis suggests that, once Q_B receives one electron from Q_A^-, D1-H252 is protonated and becomes positively charged. The protonation of the histidine can be made possible by withdrawing a proton from the nearby hydrogen bonded water molecule. The protonated D1-H252 presumably serves to stabilize the negative charge on Q_B^-. The resulting hydroxyl anion is thought to either diffuse away from the site or is protonated by other nearby water molecules if there are any. When Q_B is doubly reduced, direct protonation on Q_B^{2-} occurs in an acid/base mechanism, in which the δ1-hydrogen of D1-H252 is donated to the nearby oxygen atom of Q_B and the ϵ2-hydrogen of D1-H252 is donated to the other oxygen atom of Q_B. This may be made possible through a proton shuttle mediated by other water molecules in the Q_B niche or simply by the vibrational motions in the plastoquinone that allow its second oxygen atom to move close enough to the ϵ2-hydrogen of D1-H252. The resulting plastoquinol (Q_BH_2) will leave the binding niche, which will then be re-occupied by another plastoquinone. The deprotonated histidine will be recovered by picking up a proton from the nearby bicarbonate, producing a carbonate anion (CO_3^{2-}), which will then leave the site to allow another bicarbonate to diffuse in. It is also likely that the carbonate anion is reprotonated from the nearby environment to recover a bicarbonate. Substitution of bicarbonate (HCO_3^-) with formate (HCO_2^-) will abolish the donation of the proton to D1-H252, resulting in an inhibition of the process of Q_B^{2-} protonation (Fig. 10B).

The hypothesis that an arginine is involved in bicarbonate binding was partially supported from the analogy found in the X-ray crystal structure of human lactoferrin, which has a (bi)carbonate binding to an iron at the active site (Anderson et al., 1989). In this protein, the (bi)carbonate is stabilized by hydrogen bonding interactions with an arginine and several other adjacent amino acid residues. A similar example is found in the X-ray crystal structure of hemoglobin and myoglobin with a formate (a bicarbonate analogue) bound to the heme iron and an arginine residue interacting with the formate (Aime et al., 1996). The involvement of histidines in the protonation after Q_B^- formation is supported by the observation that the pK_a of a PSII protein group shifts from 6.4 to 7.9 upon the formation of Q_B^- (Crofts et al., 1984). Crofts et al. (1987) had earlier suggested the role of D1-H252 as a proton donor to Q_B^{2-}. Site-directed mutagenesis on D1-H252 demonstrated a dramatic influence on the PSII electron flow (see Diner et al., 1991a, 1991b; Nixon et al., 1992). Mutational studies on the other two residues, D1-R257 and D2-K23, certainly will help further test the hypothesis. We have already constructed and characterized D1-R257E

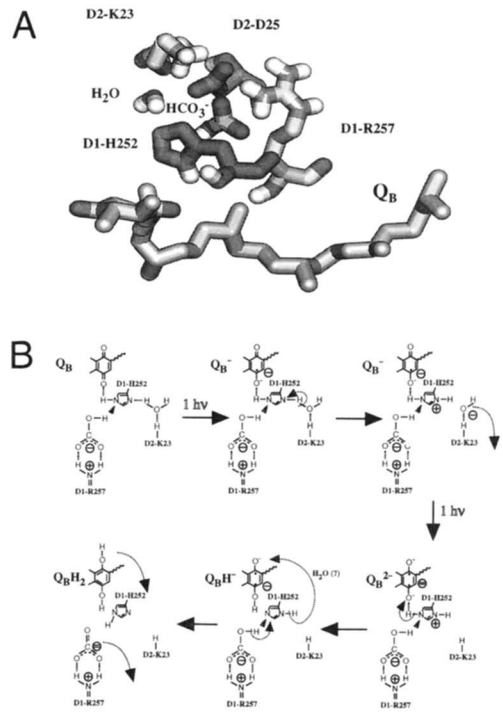

Fig. 10. A: A second bicarbonate modeled in the Q_B binding niche as an attempt to explain its involvement in Q_B protonation. A bicarbonate anion (HCO_3^-) modeled in between the side chains of D1-H252 and D1-R257 appears to be coordinated by the hydrogen bonding with the δ1-nitrogen of D1-H252 and by the hydrogen bonding/electrostatic interactions with the δ-guanido group of D1-R257. In between the imidazole group of D1-H252 and the amino group of D2-K23, a water molecule was modeled, appearing to be hydrogen bonded by both residues. Another pair of histidine/arginine close to Q_B, D1-H272/D1-R269, is also shown. D1-R269 was once proposed to be a candidate for binding bicarbonate and mediating the Q_B protonation (Govindjee and van Rensen, 1993), although its spatial position in the model appears to be unlikely for its direct involvement. **B:** A working hypothesis for the bicarbonate involvement in the protonation of Q_B. When Q_B is in the oxidized form, its carbonyl oxygen is hydrogen bonded with D1-H252 and D1-H215 (not shown). The bicarbonate and water are presumably to be anchored on D1-R257 and D2-K23, respectively, through hydrogen bonding and/or electrostatic interactions. When Q_B receives one electron from Q_A^-, D1-H252 is thought to be protonated in response to the inductive forces from the negative charge on Q_B^-. The histidine protonation can be made possible by withdrawing a proton from the nearby hydrogen bonded water molecule. The protonated D1-H252 presumably serves to stabilize the negative charge on Q_B^-. The resulting hydroxyl anion is thought to diffuse away from the site. When Q_B is doubly reduced, direct protonation on Q_B^{2-} occurs when the δ1-hydrogen of D1-H252 is donated to the nearby oxygen atom of Q_B and the ϵ2-hydrogen of D1-H252 is donated to the other oxygen atom of Q_B, which may be made possible through other water molecules or by the vibrational actions of the plastoquinone that allows its second oxygen atom to move close enough to the ϵ2-hydrogen of D1-H252. The resulting plastoquinol (Q_BH_2) will then leave the binding niche and be replaced by another plastoquinone. The deprotonated histidine will be recovered by picking up a proton from the nearby bicarbonate and producing a carbonate ion (CO_3^{2-}), which will then leave the site and be replaced by another bicarbonate. For an earlier hypothesis, see Blubaugh and Govindjee (1988a).

and D1-R257M mutants in *C. reinhardtii* and these mutants show a somewhat inhibited rate of growth and electron transfer from Q_A^- to Q_B (Q_B^-). There is a near absence of bicarbonate-reversible formate inhibition on the electron transport from Q_A^- to the plastoquinone pool, especially on the step of protonation of Q_B^{2-} (J. Xiong, J. Minagawa, A.R. Crofts, & Govindjee, unpubl. data). This evidence strongly supports the above hypothesis.

Bicarbonate/water transport in PSII

The presence of multiple water molecules in the Q_B binding region was shown experimentally in the newly refined bacterial reaction center structures (Ermler et al., 1994; Deisenhofer et al., 1995; Lancaster & Michel, 1996). In the structure of *Rb. sphaeroides*, an uninterrupted chain of fixed water molecules is found leading from the cytoplasmic surface to the Q_B molecule (Ermler et al., 1994). The water molecules in the chain are connected by hydrogen bonds to each other and to the nearby protonable residues. Their role is presumably to facilitate the protonation of doubly reduced Q_B. Some of the protonable residues that form the water channel have been confirmed to be relevant to the proton transfer process (see Lancaster et al., 1995). Interruption of the water chain near the Q_B site by site-directed mutagenesis (L-P209Y) caused a reduction of the protonation of Q_B (Bacjou & Michel, 1995).

The above experimental evidence revealed the proton transfer pathway to Q_B, which is deeply buried in the protein complex. The water-lining residues are found to be primarily charged; they are negatively charged near the Q_B niche (Ermler et al., 1994; redrawn in Fig. 11A). It is thus conceivable that bicarbonate anions will be excluded easily from the bacterial Q_B binding site due to the electrostatic repulsions. This cluster of negatively charged residues may thus help explain the fact that there is no bicarbonate effect in the bacterial reaction center.

Because the Q_B molecule in PSII is also believed to be buried inside the protein complex and its protonation must ultimately result in protons being transferred from the outer environment, it is reasonable to consider the existence of a similar transport channel, which carries protonating agents from the stroma/cytoplasm to the Q_B site. As mentioned above, the protonating agents for Q_B in PSII could be *both* water and bicarbonate.

To construct a tentative model for a similar transport channel for water and bicarbonate in PSII, we have made the following assumptions: (1) The direction of the transport channel in the PSII reaction center is similar to that in the bacterial reaction center by assuming that a good homology exists in this respect; this allows us to focus on a more specific region for constructing the model of water/bicarbonate transport. (2) The charged residues form the putative "transport channel," as in the bacterial reaction center. (3) The local electrostatic characteristic of the binding region weighs more than the precise geometric match with the bacterial water-binding residues. (4) The channel to be constructed has another end at the non-heme iron site.

In our effort to determine the location of this large bicarbonate/water binding niche or "channel" in PSII, we simply superimposed the bacterial structure (2RCR) and the constructed PSII reaction center model and identified specific D1/D2 charged residues that are positioned as in the L and M residues that form the bacterial water channel.

The following charged residues in D1 and D2 are included in the tentative transport channel: D1-H215, D1-K238, D1-E242, D1-E243, D1-E244, D1-H252, D1-R257, D1-R269, D2-K23, D2-D25, D2-E224, D2-R233, D1-E236, D2-E241, D2-E242, D2-K264, and D2-R265 (Fig. 11B). A striking feature of these charged residues is that, near Q_B and the non-heme iron, they are predominantly positively charged. This more basic Q_B/Fe binding domain is in contrast to the situation in the bacterial reaction center. This feature appears to further support the possibility of a negatively charged species, i.e., bicarbonate, to bind and function in these sites.

The available experimental evidence, that indicates the strong relevance of the above residues for binding bicarbonate/formate,

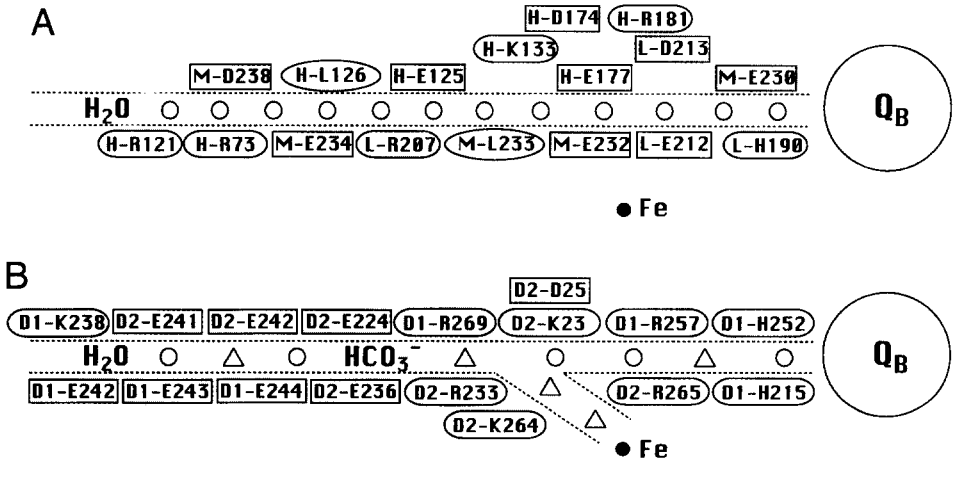

Fig. 11. A: Schematic drawing of the water chain and the surrounding amino acids in the *Rb. sphaeroides* reaction center. Water molecules presumably aid in the Q_B protonation. The polarity of the surrounding residues are boxed or circled differently. Negatively charged residues are boxed with rectangles; positively charged ones, rectangles with rounded corners; nonpolar ones, ovals (modified from Ermler et al., 1994, but with the same numbering). Several water molecules branching from the major chain and their associating amino acid residues were omitted. Water molecules are shown as small circles. **B:** Hypothetical water and bicarbonate transport channel in PSII reaction center constructed based on the assumptions made in the text. Charged residues in the PSII model considered to be important for associating with the bicarbonate and water molecules are shown. The predominately positively charged protein environment near the Q_B and the non-heme iron suggests a more favorable binding environment for bicarbonate. Water molecules are shown as small circles and bicarbonate as triangles. Residues are circled or boxed as in A.

includes results on the aforementioned D1-R257E and D1-R257M mutants (J. Xiong, J. Minagawa, A.R. Crofts, & Govindjee, unpubl. data), the D1-R269G mutant (J. Xiong, R.S. Hutchison, R.T. Sayre, & Govindjee, submitted to *Biochim. Biophys. Acta*); the D2-R233Q mutant (Cao et al., 1991) and the D2-K264 and D2-R265 mutants (see Diner et al., 1991b). These mutants, except D2-R233Q, have shown various levels of resistance to formate inhibition in support of our model. D2-R233Q was shown to be tenfold more susceptible to formate inhibition than the wild type. This can also be interpreted using the above model that the mutations resulted in a more widely "opened" transport channel, making the target site more accessible to formate. Interestingly, a deletion mutant for the above three D1 glutamate residues (D1-E242, D1-E243, and D1-E244) was also shown to be sevenfold less sensitive to formate inhibition than the wild type (Mäenpää et al., 1995). Because these are negatively charged residues, they may be more likely to serve a role for binding water molecules and providing the correct electrostatic environment in the above channel. However, the removal of the three residues results in an interruption of the transport channel and thus affects the bicarbonate/formate binding and diffusion as well.

Further mutagenesis of the arginine or lysine residues forming the "channel" by changing them to all negatively charged or neutral ones may be a good experiment to test the above hypothesis. On the other hand, mutations that change the negatively charged residues into positive ones in the "water channel" of the bacterial reaction center may serve to test the hypothesis of the above bicarbonate transport and function, provided the mutations do not introduce drastic conformational changes that seriously affect the assembly of the protein complex.

It is noted that, in the bacterial water channel, pairs of charged residues, such as L-D213/H-R181 and H-K133/H-D174, exist (Fig. 11A). This close interaction is believed to cancel the negative or positive charges on the residues and to alleviate the electrostatic repulsions (Ermler et al., 1994). Similar interactions between opposite charged residues may also exist in PSII, as predicted in the D2-K23/D2-D25 pair (Fig. 11B). In this case, the residue may bind water molecules instead.

Because the bacterial water transport channel consists of a number of residues from the H subunit, we consider that a similar situation may exist in PSII in which certain residues from other nearby PSII core polypeptides may participate in the binding of the water and bicarbonate. Because this is beyond the scope of homology modeling, we have to leave this question open.

Materials and methods

The homology modeling of the PSII reaction center of *Synechocystis* sp. PCC 6803 was performed using QUANTA/CHARMm (version 4.0) molecular modeling package. Based on the assumption that D1 is an equivalent of L and D2 is an equivalent of M, we used the coordinates of the L and M subunits from *Rb. sphaeroides* and *Rps. viridis* as the templates for D1 and D2, respectively. The coordinates of the bacterial reaction centers (1PRC and 2RCR) were obtained from the Brookhaven Protein Data Bank (Bernstein et al., 1977; Abola et al., 1987). The amino acid sequence information of D1 (from *psbA*-2) and D2 (from *psbD*-2) was obtained from Ravnikar et al. (1989) and Williams and Chisholm (1987), respectively. The posttranslational truncation on the C-terminus (16 amino acid residues) of *Synechocystis* 6803 was also taken into account (see Diner et al., 1991a).

The modeling started from the primary structure alignment of D1 and D2 with the bacterial L and M subunits, respectively. The SCRs of D1 and D2 proteins with the L or M subunits were based on the pea model by Ruffle et al. (1992). In this model, we chose to use the L subunit for aligning D1 and the M subunit for D2, respectively, rather than using all four bacterial subunits together for aligning both D1 and D2. The alignment for the sequences outside the SCRs, which are either partially conserved or structurally varied, was done on the Protein Design subprogram of QUANTA. The QUANTA alignment process is based on the multiple sequence alignment algorithm of Feng and Doolittle (1987). The alignment was done with the statistical weight for the sequence homology parameter set at 0.6. Raw alignment results were manually refined using the interactive alignment tools in the Protein Design module. After alignment, the template proteins were matched and superimposed, the coordinates of the aligned sequences were averaged and copied to the modeled sequences. The newly defined coordinates in D1 and D2 were refined with the structural regularization tool, which is a limited energy minimization function, with 50 steps using the steepest descents method followed by 200 steps of ABNR method. The regularization was conducted with less than 20 residues at a time.

Certain stretches of D1 and D2 sequences in between the aligned regions clearly do not exhibit homology with the L and M sequences. The connecting loop sequences (including the C-terminal region of D1) were treated in two different ways. For the loop sequences of less than or equal to four residues, the conformation of the loops was built using the "build coordinates" function in the protein design subprogram. The newly built peptide conformation was regularized as above. The longer loops with more than five residues were modeled with a sequence-specific approach. BLAST (Altschul et al., 1990) was applied in searching for the best-matched protein fragments among the protein sequences that already had crystal coordinates available from the Brookhaven Protein Data Bank. Once the most homologous fragment from a protein is selected, the conformation of the fragment flanked by two extra anchor residues on either end was excerpted from the original protein. Because the anchor residues of the template peptide on either side were superposed onto the two residues immediately next to the gap, the conformation of the template peptide was copied to the modeled sequences. The newly built loop conformation was then regularized as above.

The PSII chromophores, which include chlorophylls, pheophytins, and plastoquinones, were modified from their counterparts in the *Rb. sphaeroides* reaction center using the interactive graphic tools in the molecular editor function of QUANTA. The PSII chromophore structures were based on those reviewed by Cramer and Knaff (1990). The corrected PSII chromophores were then added to the assembly of D1 and D2. To accommodate the existing experimental data on the measurements of P680 chlorophyll, four alternative models of P680 conformations are proposed. One is based on the bacterial special pair, whereas the other three involve significant rotations of the two chlorophyll monomers. Because the latter three P680 conformations (see the Results and discussion) introduced enormous, unrelievable strains in the protein part of the reaction center model that had been generated by homology, they were modeled separately along with the liganding histidines and the redox active tyrosines. Another PSII chromophore, β-carotene, was also introduced into the model by modifying the dihydroneurosporene in *Rps. viridis* structure and added into the model by using the Molecular Similarity Tools in QUANTA. The non-heme

iron coordinate was transferred directly from the *Rb. sphaeroides* structure. The raw PSII reaction center complex structure was energy minimized using the CHARMm procedure (Brooks et al., 1983). The energy minimization was performed with 100 iterations of steepest descents, followed by ABNR energy minimization until fully converged (RMS force < 0.01 kcal/mol·Å), during which the coordinates of all the cofactors were constrained in place and only the D1 and D2 polypeptides could be moved. The hydrogen bonding pattern of the constructed PSII model was calculated on the protein design module and the secondary structure of D1 and D2 proteins were derived. The model was evaluated using the protein health subprogram in QUANTA and the PDF method (Subramaniam et al., 1996).

The herbicide DCMU was also modeled in the PSII reaction center, replacing Q_B in its binding niche. Its structure in *trans*-amide form was obtained by editing the phenyl ring of Q_B on the molecular editor subprogram and was added to a Q_B-lacking PSII model. The DCMU structure was moved manually to match the DCMU-binding pattern determined in the crystal structure in a mutant *Rps. viridis* reaction center (T4) (Sinning et al., 1990; Sinning, 1992). All residues surrounding DCMU were fully energy minimized with ABNR. The DCMU binding environment was further refined by molecular dynamics simulations, during which the herbicide binding environment was heated from 0 K to 300 K in 0.3 ps with an integration time of 1 fs. The structure was then equilibrated at 300 K for 25 ps with 1 fs integration time, followed by a final simulation at 300 K for 5 ps with 1 fs integration time. The structure was again fully energy minimized with ABNR. During the above energy minimization and molecular refinement processes, all the alpha-carbons of the amino acid residues were constrained so that only the residue side chains in the herbicide binding environment were allowed to move.

A bicarbonate anion (HCO_3^-) was modeled to the non-heme iron site to satisfy the iron valence requirement based on suggestions from previous experimental data (Diner & Petrouleas, 1990; Petrouleas & Diner, 1990). The docking of HCO_3^- was performed by manually placing the anion close to the Fe center and its position is compared and matched to carboxylic group of the M-E232 residue of the *Rb. sphaeroides*. A second bicarbonate, as well as a water molecule, were modeled into the Q_B niche in an attempt to study the possible involvement of bicarbonate and water in Q_B protonation. They were docked in the vicinity of D1-H252 and D1-R257 and energy minimized as above.

The entire modeling work was performed on UNIX Silicon Graphics Power Series Workstation 4D/440VGXT. Copies of the coordinates of this model in PDB format are available on request from the authors.

Acknowledgments

We thank David Tcheng for assistance in evaluating the model. The work was supported partially by an NSF grant (91-16838, supplement 1994) and a University of Illinois Research Board grant to G., and an NIH grant (GM46535) to S.S. J.X. was also supported by a training grant (DOE 92ER20095) from the Triagency (DOE/NSF/USDA) Program for Collaborative Research in Plant Biology. The computational resources were provided by the National Center for Supercomputing Applications.

References

Abola EE, Bernstein FC, Bryant SH, Koetzle TF, Weng J. 1987. Protein Data Bank. In: Allen FH, Bergerhoff G, Sievers R, eds. *Crystallographic databases—Information content, software systems, scientific applications.* Bonn/Cambridge/Chester: Data Commission of the International Union of Crystallography. pp 107–132.

Aime S, Fasano M, Paoletti S, Cutruzzolà F, Desideri A, Bolognesi M, Rizzi M, Ascenzi P. 1996. Structural determinants of fluoride and formate binding to hemoglobin and myoglobin: Crystallographic and ^{1}H-NMR relaxometric study. *Biophys J 70*:482–488.

Altschul SF, Gish W, Miller W, Myers EW, Lipman DJ. 1990. Basic local alignment search tool. *J Mol Biol 215*:403–410.

Anderson BF, Baker HM, Norris GE, Rice DW, Baker EN. 1989. Structure of human transferrin: Crystallographic structure analysis and refinement at 2.8 Å resolution. *J Mol Biol 209*:711–734.

Astashkin AV, Kawamori A, Kodera Y, Kuroiwa S, Akabori K. 1995. An electron spin echo envelope modulation study of the primary acceptor quinone in Zn-substituted plant photosystem II. *J Chem Phys 102*:5583–5597.

Astashkin AV, Kodera Y, Kawamori A. 1994. Distance between tyrosines Z^+ and D^+ in plant photosystem II as determined by pulsed EPR. *Biochim Biophys Acta 1187*:89–93.

Babcock GT. 1995. The oxygen-evolving complex in photosystem II as a metalloradical enzyme. In: Mathis P, ed. *Photosynthesis: From light to biosphere, vol II.* Dordrecht: Kluwer Academic Publishers. pp 209–215.

Bacjou L, Michel H. 1995. Role of the water chain in the reaction center from *Rb. sphaeroides*. In: Mathis P, ed. *Photosynthesis: From light to biosphere, vol I.* Dordrecht: Kluwer Academic Publishers. pp 683–686.

Barber J, Chapman DJ, Telfer A. 1987. Characterization of a PSII reaction centre isolated from the chloroplasts of *Pisum sativum*. *FEBS Lett 220*:67–73.

Bernstein FC, Koetzle TF, Williams GJB, Meyers EF Jr, Brice MD, Rodgers JR, Kennard O, Shimanouchi T, Tasumi M. 1977. The Protein Data Bank: A computer-based archival file for macromolecular structures. *J Mol Biol 112*:535–542.

Blubaugh DJ, Govindjee. 1988a. The molecular mechanism of the bicarbonate effect at the plastoquinone reductase site of photosynthesis. *Photosyn Res 19*:85–128.

Blubaugh DJ, Govindjee. 1998b. Kinetics of the bicarbonate effect and the number of bicarbonate-binding sites in thylakoid membranes. *Biochim Biophys Acta 936*:208–214.

Boekema EJ, Hankamer B, Bald D, Kruip J, Nield J, Boonstra AF, Barber J, Rogner M. 1995. Supramolecular structure of the photosystem II complex from green plants and cyanobacteria. *Proc Natl Acad Sci USA 92*:175–179.

Bosch MK, Proskuryakov II, Gast P, Hoff AJ. 1995. Relative orientation of the optical transition dipole and triplet axes of the photosystem II primary donor. A magnetophotoselection study. *J Phys Chem 99*:15310–15316.

Bowyer J, Hilton JM, Whitelegge J, Jewess P, Camilleri P, Crofts A, Robinson H. 1990. Molecular modelling studies on the binding of phenylurea inhibitors to the D1 protein of photosystem II. *Z Naturforsch 45c*:379–387.

Breton J. 1990. Orientation of the pheophytin primary electron acceptor and of the cytochrome *b*-559 in the D1–D2 photosystem II reaction center. In: Jortner J, Pullman B, eds. *Perspectives in photosynthesis*. Dordrecht: Kluwer Academic Publishers. pp 23–28.

Brooks BR, Bruccoleri RE, Olafson BD, States DJ, Swaminathan S, Karplus M. 1983. CHARMm: A program for macromolecular energy, minimization, and dynamics calculations. *J Comput Chem 4*:187–217.

Bunker G, Stern EA, Blankenship RE, Parson WW. 1982. An X-ray absorption study of the iron site in bacterial photosynthetic reaction centers. *Biophys J 37*:539–551.

Cao J, Ohad N, Hirschberg J, Xiong J, Govindjee. 1992. Binding affinity of bicarbonate and formate in herbicide-resistance D1 mutants of *Synechococcus* sp. PCC 7942. *Photosyn Res 34*:397–408.

Cao J, Vermaas WFJ, Govindjee. 1991. Arginine residues in the D2 polypeptide may stabilize bicarbonate binding photosystem II of *Synechocystis* sp. PCC 6803. *Biochim Biophys Acta 1059*:171–180.

Chang HC, Jankowiak R, Reddy NRS, Yocum CF, Picorel R, Seibert M, Small GJ. 1994. On the question of the chlorophyll *a* content of the photosystem II reaction center. *J Phys Chem 98*:7725–7735.

Chu HA, Nguyen AP, Debus RJ. 1995. Amino acid residues that influence the binding of manganese or calcium to photosystem II. 1. The lumenal interhelical domains of the D1 polypeptide. *Biochemistry 34*:5839–5858.

Clarke AK, Soitamo A, Gustafsson P, Öquist G. 1993. Rapid interchange between two distinct forms of cyanobacterial photosystem II reaction-center protein D1 in response to photoinhibition. *Proc Natl Acad Sci USA 90*:9973–9977.

Coleman WJ, Govindjee. 1987. A model for the mechanism of chloride activation of oxygen evolution in photosystem II. *Photosyn Res 13*:199–223.

Cramer WA, Knaff DB. 1990. *Energy transduction in biological membranes. A textbook of bioenergetics*. New York: Springer-Verlag. pp 194–195; 253.

Crofts AR, Robinson HH, Andrews K, van Doren S, Berry ED. 1987. Catalytic site for reduction and oxidation of quinones. In: Papa S, Chance B, Ernster L. eds. *Cytochrome systems*. New York: Plenum Press. pp 617–624.

Crofts AR, Robinson HH, Snozzi M. 1984. Reactions of quinones at catalytic sites;

a diffusional role in H-transfer. In: Sybesma C, ed. *Advances in photosynthesis research*. Hague: Martinus Nijhoff/Dr W. Junk Publishers. pp 461–468.
Debus R. 1992. The manganese and calcium ions of photosynthetic oxygen evolution. *Biochim Biophys Acta 1102*:269–352.
Debus R, Barry BA, Babcock GT, McIntosh L. 1988a. Site-directed mutagenesis identifies a tyrosine radical in the photosynthetic oxygen-evolving system. *Proc Natl Acad Sci USA 85*:427–430.
Debus R, Barry BA, Sithole I, Babcock GT, McIntosh L. 1988b. Directed mutagenesis indicates that the donor to $P680^+$ in photosystem II is tyrosine-161 of the D1 polypeptide. *Biochemistry 27*:9071–9074.
Deisenhofer J, Epp O, Sinning I, Michel H. 1995. Crystallographic refinement at 2.3-angstrom resolution and refined model of the photosynthetic reaction centre from *Rhodopseudomonas viridis*. *J Mol Biol 246*:429–457.
Diner BA, Babcock GT. 1996. Structure, dynamics, and energy conversion efficiency in photosystem II. In: Ort DR, Yocum CF, eds. *Oxygenic photosynthesis: The light reactions*. Dordrecht: Kluwer Academic Publishers. Forthcoming.
Diner BA, Nixon PJ, Farchaus JW. 1991a. Site-directed mutagenesis of photosynthetic reaction centers. *Curr Opin Struct Biol 1*:546–554.
Diner BA, Petrouleas V. 1987. Q_{400}, the non-heme iron of the photosystem II iron-quinone complex. A spectroscopic probe of quinone and inhibitor binding to the reaction center. *Biochim Biophys Acta 895*:107–125.
Diner BA, Petrouleas V. 1990. Formation by NO of nitrosyl adducts of redox components of the photosystem II reaction center. II. Evidence that HCO_3^-/CO_2 binds to the acceptor-side non-heme iron. *Biochim Biophys Acta 1015*:141–149.
Diner BA, Petrouleas V, Wendoloski JJ. 1991b. The iron-quinone electron–acceptor complex of photosystem II. *Physiol Plant 81*:423–436.
Draber W, Hilp U, Likusa H, Schindler M, Trebst A. 1993. Inhibition of photosynthesis by 4-nitro-6-alkylphenols: Structure–activity studies in wild type and five mutants of *Chlamydomonas reinhardtii*. *Z Naturforsch 48c*:213–223.
Durrant JR, Klug DR, Kwa SLS, Vangrondelle R, Porter G, Dekker JP. 1995. A multimer model for P680, the primary electron donor of photosystem II. *Proc Natl Acad Sci USA 92*:4798–4802.
Eaton-Rye JJ, Govindjee. 1988a. Electron transfer through the quinone acceptor complex of photosystem II in bicarbonate-depleted spinach thylakoid membranes as a function of actinic flash number and frequency. *Biochim Biophys Acta 935*:237–247.
Eaton-Rye JJ, Govindjee. 1988b. Electron transfer through the quinone acceptor complex II after one or two actinic flashes in bicarbonate-depleted spinach thylakoid membranes. *Biochim Biophys Acta 935*:248–257.
Egner U, Hoyer GA, Saenger W. 1993. Modeling and energy minimization studies on the herbicide binding protein (D1) in photosystem II of plants. *Biochim Biophys Acta 1142*:106–114.
El-Shintinawy F, Govindjee. 1990. Bicarbonate effects in leaf discs from spinach. *Photosyn Res 24*:189–200.
Ermler U, Fritzsch G, Buchanan SK, Michel H. 1994. Structure of the photosynthetic reaction centre from *Rhodobacter sphaeroides* at 2.65 Å resolution: Cofactors and protein-cofactor interactions. *Structure 2*:925–936.
Feng DF, Doolittle RF. 1987. Progressive sequence alignment as a prerequisite to correct phylogenetic trees. *J Mol Evol 25*:351–360.
Ghanotakis DF, Yocum CF. 1990. Photosystem II and the oxygen-evolving complex. *Annu Rev Plant Physiol Plant Mol Biol 41*:255–276.
Gilchrist ML Jr, Ball JA, Randall DW, Britt D. 1995. Proximity of the manganese cluster of photosystem II to the redox-active tyrosine Y_Z. *Proc Natl Acad Sci USA 92*:9545–9549.
Giorgi LB, Nixon PJ, Merry SAP, Joseph DM, Durrant JR, Rivas JD, Barber J, Porter G, Klug DR. 1996. Comparison of primary charge separation in the photosystem II reaction center complex isolated from wild-type and D1-130 mutants of the cyanobacterium *Synechocystis* PCC 6803. *J Biol Chem 271*:2093–2101.
Gounaris K, Chapman DJ, Booth P, Crystall B, Giorgi LB, Klug DR, Porter G, Barber J. 1990. Comparison of D1/D2/cytochrome *b*559 reaction centre complex of photosystem two isolated by two different methods. *FEBS Lett 265*:88–92.
Govindjee. 1993. Bicarbonate-reversible inhibition of plastoquinone reductase in photosystem II. *Z Naturforsch 48c*:251–258.
Govindjee, Eggenberg P, Pfister K, Strasser RJ. 1992. Chlorophyll a fluorescence decay in herbicide-resistant D1 mutants of *Chlamydomonas reinhardtii* and the formate effect. *Biochim Biophys Acta 1101*:353–358.
Govindjee, Schwarz B, Rochaix JD, Strasser RJ. 1991. The herbicide-resistant D1 mutants L275F of *Chlamydomonas reinhardtii* fails to show the bicarbonate-reversible formate effect on chlorophyll a fluorescence transients. *Photosyn Res 27*:199–208.
Govindjee, van Rensen JJS. 1993. Photosystem II reaction center and bicarbonate. In: Deisenhofer J, Norris JR, eds. *The photosynthetic reaction center, vol I*. San Diego: Academic Press. pp 357–389.
Govindjee, Vernotte C, Peteri B, Astier B, Etienne AL. 1990. Differential sensitivity of bicarbonate-reversible formate effects on herbicide-resistant mutants of *Synechocystis* 6714. *FEBS Lett 267*:273–276.
Han KF, Baker D. 1996. Global properties of the mapping between local amino acid sequence and local structure in proteins. *Proc Natl Acad Sci USA 93*:5814–5818.
Hansson O, Wydrzynski T. 1990. Current perceptions of photosystem II. *Photosyn Res 23*:131–162.
He WZ, Newell WR, Haris PI, Chapman D, Barber J. 1991. Protein secondary structure of the isolated photosystem II reaction center and conformational changes studied by Fourier transform infrared spectroscopy. *Biochemistry 30*:4552–4559.
Hienerwadel R, Berthomieu C. 1995. Bicarbonate binding to the non-heme iron of photosystem II investigated by Fourier transform infrared difference spectroscopy and ^{13}C-labeled bicarbonate. *Biochemistry 34*:16288–16297.
Hirsch DJ, Brudvig GW. 1993. Long-range electron spin–spin interactions in the bacterial photosynthetic reaction center. *J Phys Chem 97*:13216–13222.
Hoganson CW, Babcock GT. 1989. Redox cofactor interactions in photosystem II: Electron spin resonance spectrum of P_{680}^+ is broadened in the presence of Y_Z^+. *Biochemistry 28*:1448–1454.
Holzenburg A, Bewley MC, Wilson FH, Nicholson WV, Ford RC. 1993. Three-dimensional structure of photosystem II. *Nature 363*:470–472.
Hutchison RS, Xiong J, Sayre RT, Govindjee. 1996. Construction and characterization of a D1 (arginine 269-glycine) mutant of *Chlamydomonas reinhardtii*. *Biochim Biophys Acta*. Forthcoming.
Jursinic PA, Dennenberg RJ. 1990. Oxygen release time in leaf discs and thylakoids of peas and photosystem II membrane fragments of spinach. *Biochim Biophys Acta 1020*:195–206.
Kless H, Oren-Shamir M, Ohad I, Edelman M, Vermaas WFJ. 1993. Protein modifications in the D2 protein of photosystem II affect properties of the Q_B/herbicide-binding environment. *Z Naturforsch 48c*:185–190.
Klimov VV, Allakhverdiev SI, Feyziev YM, Baranov SV. 1995. Bicarbonate requirement for the donor side of photosystem II. *FEBS Lett 363*:251–255.
Kobayashi M, Maeda H, Watanabe T, Nakane H, Satoh K. 1990. Chlorophyll *a* and β-carotene content in the D_1/D_2/cytochrome *b*559 reaction center complex from spinach. *FEBS Lett 260*:138–140.
Kodera Y, Hara H, Astashkin AV, Kawamori A, Ono-TA. 1995. EPR Study of trapped tyrosine Z(+) in Ca-depleted photosystem II. *Biochim Biophys Acta 21*:43–51.
Kodera Y, Takura K, Kawamori A. 1992. Distance of P680 from the manganese complex in photosystem II studied by time resolved EPR. *Biochim Biophys Acta 1101*:23–32.
Koulougliotis D, Tang XS, Diner BA, Brudvig GW. 1995. Spectroscopic evidence for the symmetric location of tyrosines D and Z in photosystem II. *Biochemistry 34*:2850–2856.
Kramer DM, Roffey RA, Govindjee, Sayre RT. 1994. The At thermoluminescence band from *Chlamydomonas reinhardtii* and the effects of mutagenesis of histidine residues on the donor side of the photosystem II D1 polypeptide. *Biochim Biophys Acta 1185*:228–237.
Kulkarni RD, Golden SS. 1994. Adaptation to high light intensity in *Synechococcus* sp. strain PCC 7942—Regulation of three *psbA* genes and two forms of the D1 protein. *J Bacteriol 176*:959–965.
Kulkarni RD, Golden SS. 1995. Form II of D1 is important during transition from standard to high light intensity in *Synechococcus* sp. strain PCC 7942. *Photosyn Res 46*:435–443.
Kwa SLS, Eijckelhoff C, van Grondelle R, Dekker JP. 1994. Site-selection spectroscopy of the reaction center complex of photosystem II. 1. Triplet-minus absorption difference: Search for a second exciton band of P-680. *J Phys Chem 98*:7702–7711.
Lancaster CR, Ermler U, Michel H. 1995. The structures of photosynthetic reaction centers from purple bacteria as revealed by X-ray crystallography. In: Blankenship RE, Madigan MT, Bauer CE, eds. *Anoxygenic photosynthetic bacteria*. Dordrecht: Kluwer Academic Publishers. pp 503–526.
Lancaster CR, Michel H. 1996. Three-dimensional structures of photosynthetic reaction centers. *Photosyn Res 48*:65–74.
Lorkovic ZJ, Schroeder WP, Pakrasi HB, Irrgang KD, Herrman RG, Oelmueller R. 1995. Molecular characterization of PsbW, a nuclear-encoded component of the photosystem II reaction center complex in spinach. *Proc Natl Acad Sci USA 92*:8930–8934.
Mackay SP, O'Malley PJ. 1993a. Molecular modelling of the interaction between DCMU and the Q_B-binding site of photosystem II. *Z Naturforsch 48c*:191–198.
Mackay SP, O'Malley PJ. 1993b. Molecular modelling of interactions between optically active triazine herbicide and photosystem II. *Z Naturforsch 48c*:474–481.
Mackay SP, O'Malley PJ. 1993c. Molecular modelling of interactions of cyano-

acrylate inhibitors with photosystem II. Part 1. The effects of hydrophobicity of inhibitor binding. *Z Naturforsch 48c*:773–781.

Mackay SP, O'Malley PJ. 1993d. Molecular modelling of the interactions of cyanoacrylate inhibitors with photosystem II. Part 2. The effects of stereochemistry of inhibitor binding. *Z Naturforsch 48c*:782–787.

Mäenpää P, Miranda T, Tyystjärvi E, Tyystjärvi T, Govindjee, Ducruet JM, Etienne AL, Kirilovsky D. 1995. A mutation in the D-de loop of D_1 modifies the stability of the $S_2Q_A^-$ and $S_2Q_B^-$ states in photosystem II. *Plant Physiol 107*:187–197.

Maróti P, Wraight CA. 1988. Flash-induced H^+ binding by bacterial photosynthetic reaction centers: Influences of the redox states of the acceptor quinones and primary donor. *Biochim Biophys Acta 934*:329–347.

McPherson PA, Okamura MY, Feher G. 1988. Light-induced proton uptake by photosynthetic reaction centers from *Rhodobacter sphaeroides* R-26. I. Protonation of the one-electron states $D^+Q_A^-$, DQ_A^-, $D^+Q_AQ_B^-$ and $DQ_AQ_B^-$. *Biochim Biophys Acta 934*:384–368.

Metz JG, Nixon PJ, Rogner M, Brudvig GW, Diner BA. 1989. Directed alteration of the D1 polypeptide of photosystem II: Evidence that tyrosine-161 is the redox component, Z, connecting the oxygen-evolving complex to the primary electron donor, P680. *Biochemistry 28*:6960–6969.

Michel H, Deisenhofer J. 1988. Relevance of the photosynthetic reaction center from purple bacteria to the structure of photosystem II. *Biochemistry 27*: 1–7.

Nanba O, Satoh K. 1987. Isolation of photosystem II reaction center consisting of D1 and D2 polypeptides and cytochrome *b*-559. *Proc Natl Acad Sci USA 84*:109–112.

Nixon PJ, Chisholm DA, Diner BA. 1992. Isolation and functional analysis of random and site-directed mutants for photosystem II. In: Shewry P, Gutteridge S, eds. *Plant protein engineering*. Cambridge: Cambridge University Press. pp 93–141.

Nixon PJ, Diner BA. 1992. Aspartate 170 of the photosystem II reaction center polypeptide D1 is involved in the assembly of the oxygen-evolving manganese cluster. *Biochemistry 31*:942–948.

Nixon PJ, Diner BA. 1994. Analysis of water-oxidation mutants constructed in the cyanobacterium *Synechocystis* sp. PCC 6803. *Biochem Soc Trans 22*:338–343.

Noguchi T, Inoue Y, Satoh K. 1993. FT-IR studies of the triplet state of P_{680} in the photosystem II reaction center: Triplet equilibrium within a chlorophyll dimer. *Biochemistry 32*:7186–7195.

Nugent JHA, Bratt PJ, Evans MCW, MacLachlan DJ, Rigby SEJ, Ruffle SV, Turconi S. 1994. Photosystem II electron transfer: The manganese complex to P680. *Biochem Soc Trans 22*:327–331.

Oettmeier W. 1992. Herbicides of photosystem II. In: Barber J, ed. *The photosystems: Structure, function and molecular biology*. Amsterdam: Elsevier. pp 349–408.

Ohad N, Keasar C, Hirschberg J. 1992. Molecular modeling of the plastoquinone (Q_B) binding site in photosystem II. In: Murata N, ed. *Research in photosynthesis, vol II*. Dordrecht: Kluwer Academic Publishers. pp 223–226.

Okamura MY, Feher G. 1995. Proton-coupled electron transfer reactions of Q_B in reaction centers from photosynthetic bacteria. In: Blankenship RE, Madigan MT, Bauer CE, eds. *Anoxygenic photosynthetic bacteria*. Dordrecht: Kluwer Academic Publishers. pp 577–594.

Petrouleas V, Diner B. 1990. Formation of NO of nitrosyl adducts of redox components of the photosystem II reaction center. I. NO binds to the acceptor-side non-heme iron. *Biochim Biophys Acta 1015*:131–140.

Plato M, Michel-Beyerle ME, Bixon M, Jortner J. 1989. On the role of tryptophan as a superexchange mediator for quinone reduction in photosynthetic reaction centers. *FEBS Lett 249*:70–74.

Ramachandran GN, Ramakrishnan C, Sasisekharan V. 1963. Stereochemistry of polypeptide chain configurations. *J Mol Biol 7*:95–99.

Ravnikar P, Debus R, Sevrinck J, Saetaert P, McIntosh L. 1989. Nucleotide sequence on a second *psbA* gene from the unicellular cyanobacterium *Synechocystis* 6803. *Nucleic Acids Res 17*:3991.

Renger G. 1993. Water cleavage by solar radiation—An inspiring challenge of photosynthesis research. *Photosyn Res 38*:229–247.

Roffey RA, Kramer DM, Govindjee, Sayre RT. 1994. Lumenal side histidine mutations in the D1 protein of photosystem II affect donor side electron transfer in *Chlamydomonas reinhardtii*. *Biochim Biophys Acta 1185*:257–270

Ruffle SV, Donnelly D, Blundell TL, Nugent JHA. 1992. A three-dimensional model of the photosystem II reaction centre of *Pisum sativum*. *Photosyn Res 34*:287–300.

Santini C, Tidu V, Tognon G, Ghiretti Magaldi A, Bassi R. 1994. Three-dimensional structure of the higher-plant photosystem II reaction centre and evidence for its dimeric organization in vivo. *Eur J Biochem 221*:307–315.

Satoh K. 1993. Isolation and properties of the photosystem II reaction center. In: Deisenhofer J, Norris JR, eds. *The photosynthetic reaction center*. New York: Academic Press. pp 289–318.

Sayre RT, Anderson B, Bogorad L. 1986. The topology of a membrane protein: The orientation of the 32kd Q_B-binding chloroplast thylakoid membrane protein. *Cell 47*:601–608.

Schelvis JPM, van Noort PI, Aartsma, TJ, van Gorkom HJ. 1994. Energy transfer, charge separation and pigment arrangement in the reaction center of photosystem II. *Biochim Biophys Acta 1184*:242–250.

Semin BK, Loviagina ER, Aleksandrov AY, Kaurov YN, Novakova AA. 1990. Effect of formate on Mössbauer parameters of the non-heme iron of PSII particles of cyanobacteria. *FEBS Lett 270*:184–186.

Shopes RJ, Blubaugh D, Wraight C, Govindjee. 1989. Absence of a bicarbonate-depletion effect in electron transfer between quinones and reaction centers of *Rhodobacter sphaeroides*. *Biochim Biophys Acta 974*:114–118.

Shuvalov VA, Heber U, Schreiber U. 1989. Low temperature photochemistry and spectral properties of a photosystem-2 reaction center complex containing the proteins D1 and D2 and 2 hemes of Cyt *b*-559. *FEBS Lett 258*:27–31.

Sinning I. 1992. Herbicide binding in the bacterial photosynthetic reaction center. *Trends Biochem Sci 17*:150–154.

Sinning I, Koepke J, Michel H. 1990. Recent advances in the structure analysis of *Rhodopseudomonas viridis* reaction center mutants. In: Michel-Beyerle ME, ed. *Reaction centres of photosynthetic bacteria, vol 6*. Berlin: Springer-Verlag. pp 199–208.

Sinning I, Michel H, Mathis P, Rutherford AW. 1989. Characterization of four herbicide-resistant mutants of *Rhodopseudomonas viridis* by genetic analysis, electron paramagnetic resonance, and optical spectroscopy. *Biochemistry 28*:5544–5553.

Sobolev V, Edelman M. 1995. Modeling the Quinone-B binding site of the photosystem-II reaction center using notions of complementarity and contact-surface between atoms. *Proteins Struct Funct Genet 21*:214–225.

Srivastava A, Strasser RJ, Govindjee. 1995. Polyphasic rise of chlorophyll a fluorescence in herbicide-resistant D1 mutants of *Chlamydomonas reinhardtii*. *Photosyn Res 43*:131–141.

Stemler A, Jursinic P. 1993. Oxidation-reduction potential dependence of formate binding to photosystem II in maize thylakoids. *Biochim Biophys Acta 1183*:269–280.

Strasser RJ, Eggenberg P, Pfister K, Govindjee. 1992. An equilibrium model for electron transfer in photosystem II acceptor complex: An application to *Chlamydomonas reinhardtii* cells of D1 mutants and those treated with formate. *Arch Sci Gen 45*:207–224.

Subramaniam S, Tcheng DK, Fenton JM. 1996. A knowledge-based method for protein structure refinement and prediction. In: States DJ, Agarwal P, Gaasterland T, Hunter L, Smith RF, eds. *Proceedings Fourth International Conference on Intelligent Systems for Molecular Biology*. Menlo Park, California: AAAI Press. pp 218–229.

Svensson B. 1995. The photosystem II reaction centre structure, molecular modelling and experimental verification [thesis]. Stockholm, Sweden: Stockholm University.

Svensson B, Etchebest C, Tuffery P, Smith J, van Kan P, Styring S. 1995a. The structural environment of the tyrosyl radicals in photosystem II. In: Mathis P, ed. *Photosynthesis: From light to biosphere, vol I*. Dordrecht: Kluwer Academic Publishers. pp 647–650.

Svensson B, van Kan PJM, Styring S. 1995b. A proposal for the structure of the P680 pigments in photosystem II. In: Mathis P, ed. *Photosynthesis: From light to biosphere, vol I*. Dordrecht: Kluwer Academic Publishers. pp 425–430.

Svensson B, Vass I, Cedergren E, Styring S. 1990. Structure of donor side components in photosystem II predicted by computer modeling. *EMBO J 9*:2051–2059.

Svensson B, Vass I, Styring S. 1991. Sequence analysis of the D1 and D2 reaction center proteins of photosystem II. *Z Naturforsch 46c*:765–776.

Tang XS, Peloquin JM, Lorigan GA, Diner BA. 1995. The binding environment of the reduced primary quinone electron acceptor, Q_A^-, of PSII. In: Mathis P, ed. *Photosynthesis: From light to biosphere, vol I*. Dordrecht: Kluwer Academic Publishers. pp 775–778.

Taoka S, Crofts AR. 1990. Two electron gate in triazine resistant and susceptible *Amaranthus hybridus*. In: Baltscheffsky M, ed. *Current research in photosynthesis, vol 1*. Dordrecht: Kluwer Academic Publishers. pp 547–550.

Telfer A, Dhami S, Bishop SM, Phillips D, Barber J. 1994. Beta-carotene quenches singlet oxygen formed by isolated photosystem II reactions centers. *Biochemistry 33*:14469–14474.

Tietjen KG, Kluth JF, Andree R, Haug M, Lindig M, Müller KH, Wroblowsky HJ, Trebst A. 1991. The herbicide binding niche of photosystem II-a model. *Pest Sci 31*:65–72.

Trebst A. 1986. The topology of the plastoquinone and herbicide binding peptides of photosystem II-a model. *Z Naturforsch 41c*:240–245.

Trebst A. 1991. A contact site between the two reaction center polypeptides of photosystem II is involved in photoinhibition. *Z Naturforsch 46c*:557–562.

van der Vos R, van Leeuwen PJ, Braun P, Hoff AJ. 1992. Analysis of the optical absorbance spectra of D1–D2–cytochrome *b*-559 complexes by absorbance-detected magnetic resonance. Structural properties of P680. *Biochim Biophys Acta 1140*:184–198.

van Dorssen RJ, Breton J, Plijter JJ, Satoh K, van Gorkom HJ, Amesz J. 1987. Spectroscopic properties of the reaction center and of the 47 kDa chlorophyll protein of photosystem II. *Biochim Biophys Acta 893*:267–274.

van Gorkom HJ, Schelvis JPM. 1993. Kok's oxygen clock: What makes it tick? The structure of P680 and consequences of oxidizing power. *Photosyn Res 38*:297–301.

van Leeuwen PJ, Nieveen MC, van de Meent EJ, Dekker JP, van Gorkom HJ. 1991. Rapid and simple isolation of pure photosystem II core and reaction center particles from spinach. *Photosyn Res 28*:149–153.

van Mieghem FJE, Satoh K, Rutherford AW. 1991. A chlorophyll tilted 30° relative the membrane in the photosystem II reaction center. *Biochim Biophys Acta 1058*:379–385.

van Rensen JJS, Tonk WJM, de Bruijn SM. 1988. Involvement of bicarbonate in the protonation of the secondary quinone electron acceptor of photosystem II via the non-heme iron of the quinone-iron acceptor complex. *FEBS Lett 226*:347–351.

Velthuys BR. 1981. Electron dependent competition between plastoquinone and inhibitors for binding to photosystem II. *FEBS Lett 126*:277–281.

Vermaas W. 1993. Molecular-biological approaches to analyze photosystem II structure and function. *Annu Rev Plant Physiol Plant Mol Biol 44*:457–481.

Vermaas WFJ, Charité J, Shen G. 1990. Q_A binding in D2 contributes to the functional and structural stability of photosystem II. *Z Naturforsch 45c*:359–365.

Vermaas WFJ, Ikeuchi M. 1991. Photosystem II. In: Bogorad L, Vasil IK, eds. *Photosynthetic apparatus: Molecular biology and operation*. San Diego: Academic Press. pp 25–111.

Vermaas WFJ, Rutherford AW. 1984. EPR measurements on the effects of bicarbonate and triazine resistance on the acceptor side of photosystem II. *FEBS Lett 175*:243–248.

Vermaas WFJ, Rutherford AW, Hansson Ö. 1988. Site-directed mutagenesis in photosystem II of the cyanobacterium *Synechocystis* sp. PCC 6803; Donor D is a tyrosyl residue in the D2 protein. *Proc Natl Acad Sci USA 85*:8477–8481.

Vermaas WFJ, Styring S, Schröder WP, Andersson B. 1993. Photosynthetic water oxidation: The protein framework. *Photosyn Res 38*:249–263.

Vermaas WFJ, Williams JGK, Arntzen CJ. 1987. Site-directed mutations of two histidine residues in the D2 protein inactivate and destabilize photosystem II in the cyanobacterium *Synechocystis* 6803. *Z Naturforsch 42c*:762–768.

Vermaas W, Vass I, Eggers B, Styring S. 1994. Mutation of a putative ligand to the non-heme iron in photosystem II: Implications for Q_A reactivity, electron transfer, and herbicide binding. *Biochim Biophys Acta 1184*:263–272.

Vernotte C, Briantais JM, Astier C, Govindjee. 1995. Differential effects of formate in single and double mutants of D_1 in *Synechocystis* sp. PCC 6714. *Biochim Biophys Acta 1229*:296–301.

Wachtveitl J, Farchaus JW, Das R, Lutz M, Robert B, Mattioli TA. 1993. Structure, spectroscopic, and redox properties of *Rhodobacter sphaeroides* reaction centers bearing point mutations near the primary electron donor. *Biochemistry 32*:12875–12886.

Wang X, Cao J, Maroti P, Stilz HU, Finkele U, Lauterwasse C, Zinth W, Oesterhelt D, Govindjee, Wraight CA. 1992. Is bicarbonate in photosystem II the equivalent of the glutamate ligand to the iron atom in bacterial reaction center? *Biochim Biophys Acta 1100*:1–8.

Williams JGK, Chisholm DA. 1987. Nucleotide sequence of both *psbD* genes from the cyanobacterium *Synechocystis* 6803. In: Biggins J, ed. *Progress in photosynthesis research, vol IV*. Dordrecht: Martinus Nijhoff Publishers. pp 809–812.

Wincencjusz H, Allakhverdiev SI, Klimov VV, van Gorkom HJ. 1996. Bicarbonate-reversible formate inhibition at the donor side of photosystem II. *Biochim Biophys Acta 1273*:1–3.

Wraight CA. 1979. Electron acceptors of bacterial photosynthetic reaction centers. II. H^+ binding coupled to secondary electron transfer in the quinone acceptor complex. *Biochim Biophys Acta 548*:309–327.

Wraight CA. 1981. Oxidation-reduction physical chemistry of the acceptor quinone complex in bacterial photosynthetic reaction centers: Evidence for a new model of herbicide activity. *Israel J Chem 21*:348–354.

Xiong J, Hutchison RS, Sayre R, Govindjee. 1995. Characterization of a site-directed mutant (D1-arginine 269-glycine) of *Chlamydomonas reinhardtii*. In: Mathis P, ed. *Photosynthesis: From light to biosphere, vol I*. Dordrecht: Kluwer Academic Publishers. pp 525–528.

Xu C, Taoka S, Crofts AR, Govindjee. 1991. Kinetic characteristics of formate/formic acid binding at the plastoquinone reductase site in spinach thylakoids. *Biochim Biophys Acta 1098*:32–40.